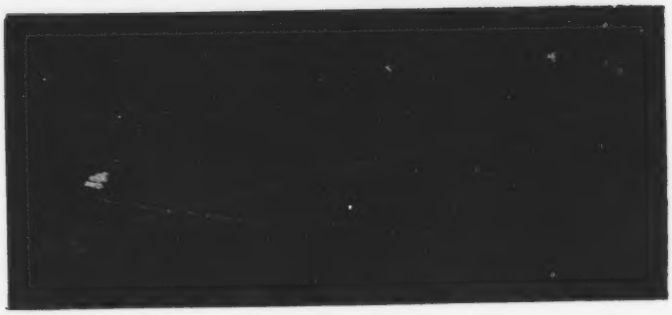

CN rail research

recherche CN rail

CN

TP 8169E 188

RESONANT VIBRATION FREQUENCIES IN CONCRETE TIES

Prepared for

TRANSPORT CANADA
TRANSPORTATION DEVELOPMENT CENTRE

Mr. A. Taras
Project Engineer

Canadian National Railways
Technical Research Centre
3950 Hickmore Ave.
St. Laurent, Quebec
H4T 1K2

December 1985

R001

The contents of this report reflect the views of the contractor and not necessarily the official views or policies of the Transportation Development Centre (TDC) of Transport Canada.

Un sommaire en français de ce rapport est inclus avant la table des matières.

Transport Canada / Transports Canada

Development / Développement

REPORT DOCUMENTATION FORM

1. Transport Canada Report No.	2. TDC Project No.	3. Recipient's Catalogue No.
TP 8169E	4929	

4. Title and Subtitle	5. Report Date
RESONANT VIBRATION FREQUENCIES IN CONCRETE TIES	December 1985
	6. Performing Organization Report No. 188
7. Author(s)	8. Transport Canada File No.
Mr. A. Taras, Project Engineer	D1465-404
9. Performing Organization Name and Address Canadian National Railways Technical Research Centre 3950 Hickmore Avenue St. Laurent, Quebec H4T 1K2	10. DSS File No. 12SD.T8200-2-2586
	11. DSS or Transport Canada Contract No. OSD83-00002
12. Sponsoring Agency Name and Address Transportation Development Centre (TDC) Guy Favreau Complex 200 Dorchester Blvd. West, Suite 601, West Tower Montreal, Quebec H2Z 1X4	13. Type of Report and Period Covered Final 1982-1984
	14. Sponsoring Agency Code
15. Supplementary Notes Canadian National Railways and TDC equally shared the cost of this program.	16. TDC Project Officer D.W. Dibble

17. Abstract

Concrete ties undergo impact loading in track and tend to oscillate at their resonant bending frequencies as a result. These rather high frequency bending fluctuations all contribute to the fatigue loading environment that the ties must endure. In order to define these frequencies, laboratory tests were conducted on CN60A, CN60B, and CN No. 20 turnout concrete ties. Based on these results, theoretical frequencies were determined for the CN modified Type A concrete bridge tie. This report documents the first four bending mode frequencies as well as the concrete damping characteristics for each of the tie types.

18. Key Words	19. Distribution Statement
Rail, Track, Concrete Ties, Resonant Bending Frequencies, Damping Characteristics	A limited number of copies are available upon request from the Transportation Development Centre

20. Security Classification (of this report)	21. Security Classification (of this page)	22. No. of Pages	23. Price
Unclassified	Unclassified	78	-

TDC. CDT 79-005
Rev 86

Canada

Transports Canada / Transport Canada
Développement / Development

FORMULE DOCUMENTAIRE DU RAPPORT

1. N° du rapport Transports Canada	2. N° de l'étude — CDT	3. N° de catalogue du destinataire
TP 8169E	4929	

4. Titre et sous-titre	5. Date du rapport
RESONANT VIBRATION FREQUENCIES IN CONCRETE TIES	décembre 1985
	6. N° du rapport de l'organisme exécutant: 188

7. Auteur(s)	8. N° de dossier Transports Canada
M. A. Taras, Ingénieur études	D1465-404

9. Nom et adresse de l'organisme exécutant	10. N° de dossier — ASC
Centre de Recherche CN Rail 3950 avenue Hickmore St. Laurent (Québec) H4T 1K2	12SD.T8200-2-2586
	11. N° de contrat — ASC ou Transports Canada: OSD83-00002

12. Nom et adresse de l'organisme parrain	13. Genre de rapport et période visée
Centre de développement des transports (CDT) Complexe Guy-Favreau 200 ouest, boul. Dorchester, Suite 601, Tour Ouest Montréal (Québec) H2Z 1X4	Final 1982-1984
	14. Code de l'organisme parrain

15. Remarques additionnelles	16. Agent de projet — CDT
Le Canadien National et le Centre de développement des transports ont partagé le coût du programme à part égale.	D.W. Dibble

17. Résumé

Les traverses en béton mises en voie sont soumises à des charges de choc qui provoquent des oscillations aux fréquences de résonance. Ces flexions à alternances plutôt rapides ajoutent aux contraintes de fatigue que les traverses doivent endurer. Dans le but de mettre en évidence les fréquences en question, des essais de laboratoire ont été faits sur les traverses de voie CN60A et CN60B et sur les traverses pour branchements CN n° 20. A partir des résultats obtenus, les fréquences de résonance de la traverse CN type A modifiée pour ponts-rails ont été déterminées par calcul. Le présent rapport concerne la recherche sur les fréquences dans les quatre premiers modes de flexion ainsi que sur les caractéristiques d'amortissement de ces quatre types de traverse en béton.

18. Mots-clés	19. Diffusion
Rail, voie, traverses en béton, fréquences de résonance en flexion, caractéristiques d'amortissement	Le Centre de développement des transports dispose d'un nombre limité d'exemplaires.

20. Classification de sécurité (de ce rapport)	21. Classification de sécurité (de cette page)	22. Nombre de pages	23. Prix
non classifié	non classifiée	78	-

EXECUTIVE SUMMARY

Wheel impact loading governs the design of concrete ties. Ties that are impacted undergo resonant bending fluctuations, meaning that they go into reverse bending and suffer far more fatigue loading cycles than those imposed by the simple passing frequency of wheels. The number of additional loading cycles is governed by the incidence of "bad" wheels, the static wheel loading, and the damping characteristics of the concrete tie, the rail/tie pad, and the ballast and roadbed. In order that all these factors be taken into account when optimizing concrete tie design, it is essential that the dynamic characteristics of the ties themselves be fully understood.

This report documents the first four resonant mode frequencies as well as the damping characteristics of four concrete tie types: CN60A track tie, CN60B track tie, CN No. 20 concrete turnout tie, and CN modified Type A concrete bridge tie.

To assess the resonant frequencies and damping coefficients of the ties in the laboratory, a method was required by which these values could be determined independently of tie support conditions. In track, the support conditions vary considerably and are in general difficult to simulate. Therefore they are not suited as physical references on which to establish the tie dynamic characteristics. In order to determine the dynamic characteristics, the vibration tests were done with the ties suspended in a so-called "Free-Free" condition. This quasi-free state of dynamic motion provides for little influence from the supports on the tie vibration.

CN's Research Centre designed and constructed a test frame and conducted tests and analysis of the 4 tie types. The findings are summarized below:

- The frequency of passing wheels is much lower than that of any of the tie resonant frequencies. The ties will therefore not be forced into resonance, and they should not be subjected to destructive continuing vibrations.

- The concrete ties themselves have very low damping, but under the heavier axle loads, they are pressed tightly to the roadbed, which has much higher damping capability.

- Regular track ties (CN60A and CN60B) are deflected into their third mode shape (symmetric) under normal track loading conditions. Under impact loading from skid-flat wheels, which normally strike both rails at roughly the same time, the ties are excited at their third mode resonant frequencies (638 Hz for the CN60A tie, 603 Hz for the CN60B tie). Under heavy pressure from loaded cars, the vibrations are quickly damped by the ballast and roadbed.

- Under lightly loaded cars, the ties are not pressed as heavily into the ballast and damping will be less effective. There is an uplift wave on the rail under centres of cars (between the two trucks), and the ties are lifted free of the damping ballast pressure. Under high speed lightly loaded vehicles, the impacted ties are set up in a state of resonant vibration which is not damped out quickly by the roadbed. Sustained vibrations in the range of 640 Hz could be maintained.

- The CN bridge ties are supported by rubber pads on girders at 8 ft. spacing. The primary bending mode of the ties should therefore be the first, and there will be no damping from roadbed ballast. This will be documented in a future report covering strain gauge measurements on CN experimental bridge ties installed at mile 122.4 Drummondville Subdivision.

- The majority of the concrete turnout ties will be loaded asymmetrically on account of the divergence of tracks. The bending mode shapes that ties assume under traffic (including defective wheel impact loading) can only be determined through power spectral analysis of field measured data. This will be documented in a future report.

The frequencies, damping coefficients and flexural resonant mode shapes, documented in this report, will be useful:

i) in evaluating the performance of ties in track.

ii) in understanding the track-tie behaviour through field measurements.

iii) in finding remedies to unwanted effects such as destructive vibrations of track structure, reverse bending of ties and development of cracks, and finally,

iv) in optimizing tie designs to reduce the production costs.

SOMMAIRE

Le dimensionnement des traverses en béton est fonction des charges de choc exercées par les roues. Une traverse soumise à ce type de sollicitations est le siège de vibrations de flexion à sa fréquence de résonance qui fait qu'elle connaît des flexions négatives et subit des cycles de contrainte de fatigue en nombre beaucoup plus grand que ceux attribuables à la fréquence de passage des roues. Le nombre additionnel de cycles de charge est fonction du nombre de roues défectueuses, de la charge statique des roues et des caractéristiques d'amortissement de l'ensemble traverse/semelle/ballast/plate-forme. Afin de bien prendre en compte tous ces facteurs et déboucher sur un dimensionnement adéquat des traverses en béton, les caractéristiques dynamiques de celles-ci doivent être approfondies.

Le présent rapport donne le résultat de la recherche faite sur les fréquences dans les quatre premiers modes de vibration de flexion ainsi que sur les caractéristiques d'amortissement de quatre types de traverse en béton, à savoir CN60A et CN60B qui sont des traverses de voie, CN n° 20 traverse pour branchements et CN type A modifiée pour ponts-rails.

Dans le but de mettre en évidence en laboratoire les fréquences de résonance des traverses, et leur coefficient d'amortissement, une méthode a été étudiée pour permettre de faire abstraction des systèmes d'appui. En effet, les conditions d'appui des traverses varient considérablement dans la réalité et sont, de façon générale, difficiles à reproduire. Elles ne constituent donc pas une base de réference appropriée pour caractériser le comportement dynamique d'une traverse. Pour les essais vibratoires, les traverses ont été suspendues dans des conditions dites libre-libre ou de mouvement dynamique quasi-libre, où l'influence des appuis sur le comportement vibratoire est très faible.

Le Centre de recherche CN Rail a conçu et réalisé un montage d'essai approprié et il a procédé aux essais et aux analyses subséquentes concernant ces quatre types de traverses. La recherche a débouché sur les constatations suivantes:

- La fréquence de passage des roues est bien inférieure à toutes les fréquences de résonance des traverses; ces dernièrs ne sont donc pas contraintes à des vibrations forcées et entretenues pouvant conduire à leur ruine.

- L'amortissement propre des traverses considérées est très faible, mais, sous charges élevées, elles s'enfoncent dans le ballast qui présente un amortissement beaucoup plus marqué.

- Dans des conditions de charges normales, les traverses CN60A et CN60B vibrent selon le mode 3 (mode symétrique). Toutefois, sous les chocs dus à des roues défectueuses, comportant des méplats de patinage qui généralement frappent les deux rails à peu près en même temps, les traverses vibrent selon le même mode, mais à leur fréquence de résonance, soit 638 et 603 Hz pour les traverses A et B, respectivement. Au passage d'un convoi chargé, ces oscillations sont rapidement amorties par le ballast et la plate-forme.

- Au passage d'un convoi légèrement chargé, l'enfoncement dans le ballast est moins profond, de sorte que l'amortissement procuré par celui-ci n'est pas aussi efficace. Sous le centre des wagons, c'est-à-dire à mi-chemin entre les deux bogies, les traverses sont soulevées légèrement sur les rails, réduisant d'autant l'amortissement procuré par le ballast. Dans le cas d'un trafic relativement léger mais rapide, les chocs provoquent des vibrations à la fréquence de résonance qui, n'étant pas rapidement amorties par la plate-forme, provoquent à leur tour des oscillations entretenues de l'orde de 640 Hz.

- Les traverses pour pont-rail du CN s'appuient sur des semelles en caoutchouc placées directement sur les poutres à 8 pi d'intervalle. Le mode dominant de flexion devrait donc être le mode 1 et il n'y aurait pas d'amortissement procuré par le ballast. Cette recherche particulière fera l'objet d'un rapport ultérieur donnant le résultat des mesures extensométriques faites sur les traverses posées à titre expérimental par le CN au droit du mille 122,4 de la subdivision Drummondville.

- La plupart des traverses pour branchements sont soumises à des charges asymétriques à cause de la convergence des voies. La mise en évidence des formes de flexion prises par les traverses en charge, y compris les cas de charges de choc dues aux roues défectueuses, ne peut se faire que par l'analyse de la densité spectrale de puissance à partir des données enregistrées in situ. Ce sera l'objet d'un rapport ultérieur.

Les fréquences, les coefficients d'amortissement et les formes de mode résonant en flexion, dont le présent rapport fait état, permettront:

i) d'évaluer la tenue des traverses mises en voie,

ii) de connaître l'interaction rail-traverse en ligne,

iii) de remédier à certains phénomènes dangereux: vibrations destructives de la voie, flexions négatives des traverses et amorce de fissures,

iv) d'optimiser le dimensionnement des traverses pour un coût de fabrication réduit.

TABLE OF CONTENTS

		Page No.
1.	INTRODUCTION	1
2.	TEST SET-UP	2
	2.1 General Description	2
	2.2 Set-up Requirements	2
	2.3 Force Transmission Link	5
	2.4 Tie Motion Sensors	7
	2.5 Instrumentation Set-up	7
3.	TEST PROCEDURE	10
4.	MEASUREMENTS	12
	4.1 Resonant Frequencies and Modes	12
	4.2 Frequency Spectra Interpretation	12
	4.3 Computation of Damping Coefficient	13
5.	ANALYSIS OF TEST RESULTS	14
	5.1 Track Tie Data: CN60A,CN60B	14
	5.2 Switch Tie Data	15
6.	ANALYTICAL PREDICTION OF FREQUENCIES	19
7.	THEORETICAL EVALUATION OF BRIDGE TIE FREQUENCIES	21
8.	DISCUSSION OF TEST RESULTS	22
	8.1 Frequencies	22
	8.2 Damping	22
	8.3 Theoretical Prediction	23
	8.4 Comparison between Analytical and Field Results	24
9.	GENERAL DISCUSSION	25
10.	CONCLUSIONS	27
11.	RECOMMENDATIONS	28
APPENDIX No. 1	THEORETICAL EQUATIONS	35
APPENDIX No. 2	TIE CENTROID LOCATION	38
APPENDIX No. 3	TIE MOMENT OF INERTIA	41
APPENDIX No. 4	DYNAMIC TEST DATA FOR CN60A, CN60B, CN No. 20 TURNOUT TIES	44
APPENDIX No. 5	FREQUENCY RESPONSE PLOTS OF CN60A, CN60B, CN No. 20 TURNOUT TIES	48

LIST OF FIGURES

		Page No.
1.	Schematic Tie Vibration Test Arrangement.....	3
2.	Set-up Suspension for 8'-3" Track Tie.....	4
3.	Set-up Suspension for 10'-6" Switch Tie.....	4
4.	Force Transmission Link.....	6
5.	Accelerometer Locations on Track Tie.....	8
6.	Accelerometer Locations on ST-49 Switch Tie.....	8
7.	Instrumentation Layout.....	9
8.	Frequencies of Concrete Switch Ties.....	18
9.	Description of CN60A Concrete Track Tie.....	29
10.	Description of CN60B Concrete Track Tie.....	30
11.	Description of CN Concrete Switch Tie.....	31
12.	Description of CN Type A Concrete Bridge Tie.....	32
13.	Accelerometer Stations for CN60A and B Ties.....	33
14.	Accelerometer Positions for 10'-6" Switch Tie.....	34
15.	Spectral Analysis of CN60A Tie: A- Magnitude.....	49
	B- Phase.....	50
16.	Spectral Analysis of CN60B Tie: A- Magnitude.....	51
	B- Phase.....	52
17.	Spectral Analysis of CN No. 20 Turnout Tie: A- Magnitude..	53
	B- Phase.....	54
18.	Spectral Analysis of CN60B Tie, 1st mode: A- Magnitude....	55
	B- Phase.....	56
19.-	Spectral Analysis of CN60B Tie, 2nd mode: A- Magnitude....	57,59
20.	B- Phase.....	58,60
21.-	Spectral Analysis of CN60B Tie, 3rd mode: A- Magnitude	61,63
22.	B- Phase.....	62,64
23.	Spectral Analysis of CN60B Tie, Higher Mode: A- Magnitude.	65
	B- Phase.....	66
24.	Spectral Analysis of CN Bridge Tie Field Response.....	67

LIST OF TABLES

		Page No.
1.	Mode Characteristics of CN60A Tie.....	16
2.	Mode Characteristics of CN60B Tie.....	16
3.	Mode Characteristics of CN ST-49 Turnout Tie.....	17
4.	Mode Characteristics of CN Bridge Tie (Theoretical).....	17
5.	Comparative Table of Test and Predicted Frequencies for 10'-6" Switch Tie.....	20
6.	Dynamic Test Data for CN60A Tie.....	45
7.	Dynamic Test Data for CN60B Tie.....	46
8.	Dynamic Test Data for CN Concrete Switch Tie.....	47

1. INTRODUCTION

This investigation was conducted by Canadian National Railways Research Department to determine the dynamic characteristics (resonant frequencies, internal damping) of concrete ties.

It was prompted by the need to have a more rational basis on which to compare the actual physical behaviour of the different concrete tie designs that CN Rail currently has in service.

Concrete ties live in a fatigue loading environment with dynamic impacts, and for an optimization of tie design it is imperative to consider the dynamic characteristics.

They will be complementary to the static strength characteristics already established in the laboratory.

To assess the resonant frequencies and damping coefficients of the ties in the laboratory, a method was required by which these values could be determined independently of tie support conditions. In track, the support conditions vary considerably and are in general difficult to simulate. Therefore they are not suited as physical references on which to establish the tie dynamic characteristics. In order to determine the dynamic characteristics, the vibration tests were done with the ties suspended in a so-called "Free-Free" condition, as shown in Figure No. 1. This quasi-free state of dynamic motion provides for little influence from the supports on the tie vibration. For this purpose, CN Research Centre designed and constructed a test frame and conducted tests and analysis described in the following sections.

The objectives of this work were to determine:

1- the resonant frequencies of the ties
2- the resonant modes of bending of the ties
3- the damping coefficients at resonance

for four CN concrete ties: CN60A, CN60B, CN Turnout ties and Bridge ties, (see Figures 9 to 12).

This data would hopefully serve, combined with the static structural characteristics, to complete the data base for evaluation of the performance of ties in track.

Also the information would increase the understanding of track-tie behaviour and subsequently of the cause of unwanted effects such as resonant vibrations of track structure leading to reverse bending of ties and fatigue cracks.

2. TEST SET-UP

2.1 General Description

A schematic of the concrete tie vibration arrangement is illustrated in Figure No. 1. It consisted of an A frame, 15 ft. high, supporting two electric hoists which were free to move on rollers, along the top horizontal beam. Their hooks were attached to a system of springs which were in turn hooked to two shoulders of the tie, (both symmetric about the tie center).

Through this system, it was possible to raise the tie off its supports, into a softly suspended position. Also it permitted positioning the electro-dynamic shaker unerneath the tie at a suitable location, and through a link between the tie and shaker, to generate vibrations in the tie.,

2.2 Set-up Requirements

To obtain dynamic characteristics representative of the beam alone, a "Free-Free" state of vibration of the concrete tie had to be achieved, or a state as close to it as possible. This arrangement would reduce the influence of the supports.

This was realized through the following conditions:

i) Very low spring-rates.

It was shown that for springs of low spring constants, the system comprising the suspended tie and the springs could be dynamically decoupled for all practical purposes. This meant that the rigid body motion of the tie on springs was negligeable compared to its flexural motion about its neutral axis.

In the following tests, two spring configurations were used:

Configuration A: Two simple springs each attached to a shoulder symmetric to the tie centre (see Figure No. 2). They were used for the track ties CN60A, CN60B. Their spring-rate and maximum load were 77 lb./in. and 500 lb., for each spring.

Configuration B: Two sets of two springs, rigged in parallel, each set attached to a shoulder approximately symmetric to the centre of the 10 ft. 6 in. CN Turnout tie (see Figure No. 3). The spring rate of each set of springs (double the rate of a simple spring) was 154 lb./in. and the maximum load per set was 1000 lb.

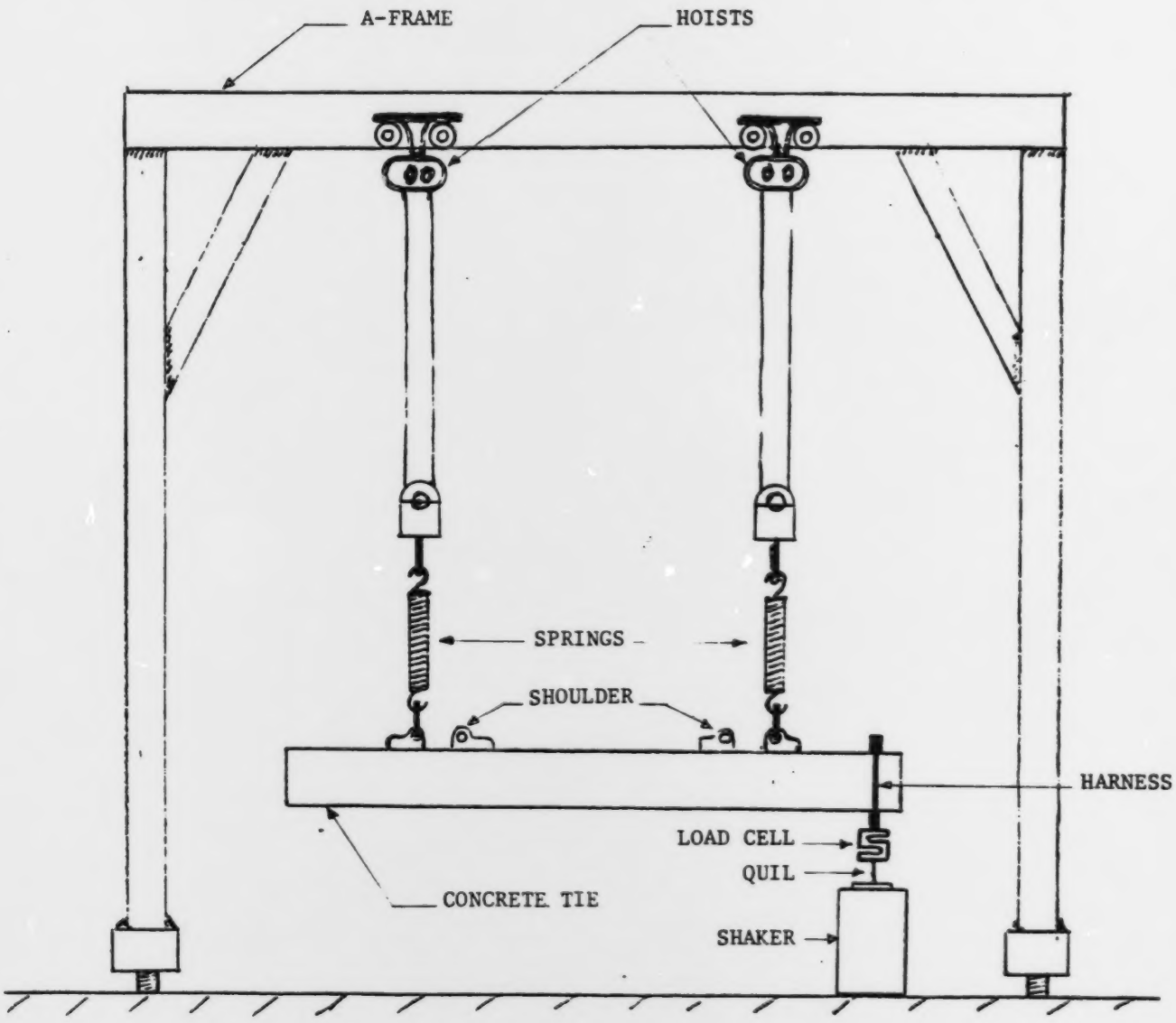

FIGURE NO. 1 SCHEMATIC TIE VIBRATION TEST ARRANGEMENT

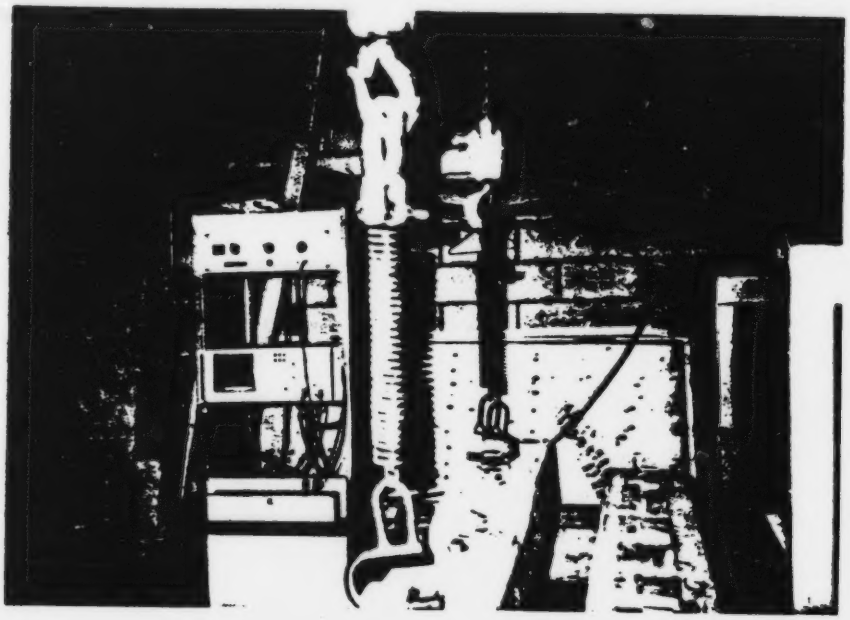

FIGURE NO. 2 SET-UP SUSPENSION FOR 8'-3" TRACK TIE

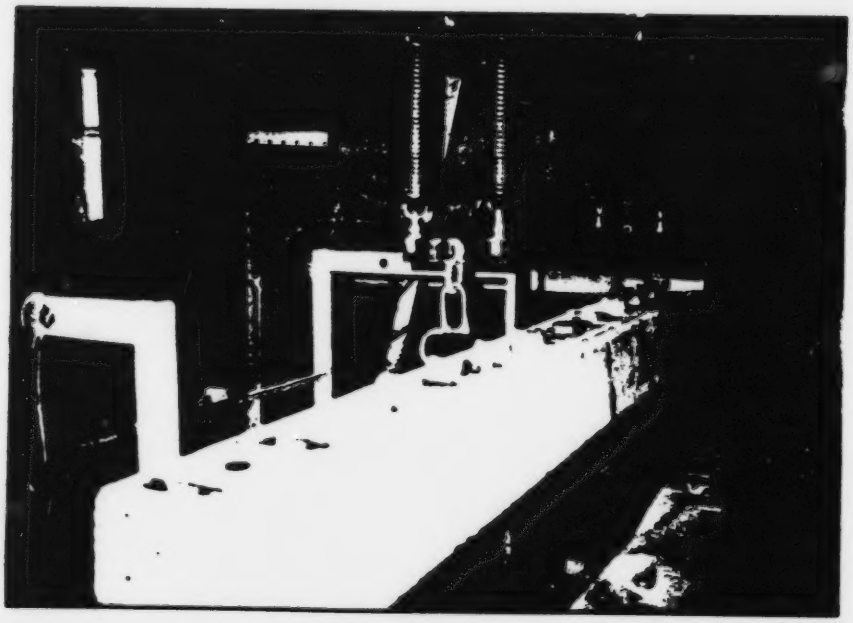

FIGURE NO. 3 SET-UP SUSPENSION FOR 10"-6" "TURNOUT TIE

ii) Long suspended length.

The way the excitation force was being applied underneath the tie created a physically unstable dynamic system. If excited at the proper frequency, (pendulum frequency equal to $\frac{1}{2\pi}\sqrt{\frac{g}{L}}$, where g is gravity and L the suspended length), a non desirable lateral motion could have been generated. Therefore the pendulum frequency was lowered below 1 Hz, out of the frequency range of tie resonances, by suspending it 15 ft down (see Figure No. 1).

iii) Location of the support points.

Also to reduce, even more, the effect of the support points on the free vibration of the ties, they were chosen at shoulders closest to the nodal points of the first resonant mode. They were located at a distance of 22% of the tie length, from either end (see Figures Nos. 2 and 3). This would eliminate the effect of the first mode which contains most of the vibratory energy.

A note of practical consideration concerning the test set-up: the set-up had to permit raising or lowering the tie to any height. It would then permit positioning the shaker underneath and permit lowering the tie close enough to the head of the shaker, to be able to link the two up.

2.3 Force Transmission Link

The excitation force was applied by the shaker to the tie at locations (A, A') and (B, B') for both track ties and only location (A, A') for the Switch Tie (see Figures Nos. 13 and 14.). This force was transmitted through a series of components which made up the force link (see Figures Nos. 4 and 5).

There was the "S" shaped load cell, used to measure the excitation force. It was a strain gauge transducer, with a sensitivity of 3 mv/v and a capacity of +100 lb. It was screwed directly to the bottom of a rigid harness made of aluminum bars and two long threaded steel rods that held the load cell tightly to the tie.

On the shaker head were two rods: one in brass attached firmly to it and another in nylon, called the Quil, that screwed freely into the brass rod. The latter could also be turned up and screwed in to the bottom of the load cell, closing the gap between the shaker and the tie (see Figure No. 4).

Note: The reason for the Quil was to avoid any damages to the load cell or shaker, due to possible lateral swaying of the tie.

Also the position of the load cell in the link was the most suited in determining, to a good approximation, the response of the tie. Because of the high rigidity between load cell and the tie, it saw for any practical purpose all the force transmitted to the tie. This would not have been the case if placed between the Quil and shaker head.

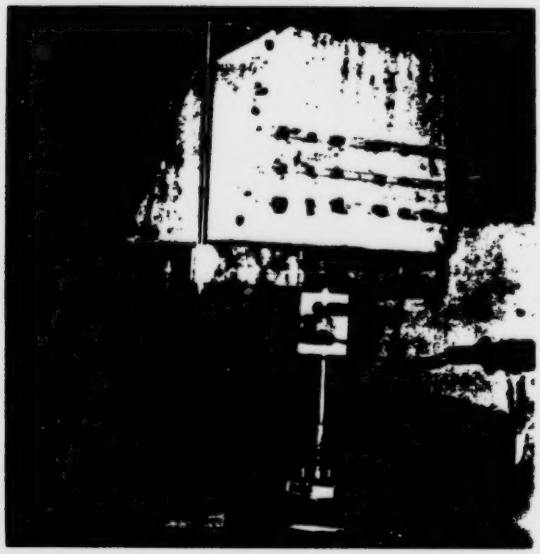

FIGURE NO. 4 FORCE TRANSMISSION LINK

In fact, the force sensed by the load cell was not exactly that which was applied to the tie, because of the mass of the harness. Nonetheless it was a good approximation in view of the ratio of the weight of the harness to the weight of the tie.

2.4 Tie Motion Sensors

The response of the ties was detected through small piezo-electric accelerometers (1 oz. weight) with a half inch diameter contact base. The accelerometer could be moved at different locations along the ties. Thirteen locations in all were determined per tie in order to get a good definition of the first three or four resonant mode shapes.

These locations were different for the CN60A and B ties (see Figures Nos. 5 and 13) compared to the No. 20 (10 ft. 6 in.) turnout tie (see Figures Nos. 6 and 14). To fix the accelerometer in place, little aluminum blocks 2 x 3/4 x 3/8 inch dimension) previously center drilled and tapped, were epoxied at the locations onto the tie, ready to have the accelerometer screwed in tightly.

2.5 Instrumentation Set Up

The instrumentation layout, as shown on Figure No. 7 presented three functional groups: -the power group
-the signal generator group
-the signal analyses group

To power up the instrumentation for the tests, there were:

- the power amplifier that energized the driving inductance coils of the shaker.
- the D.C. voltage supply that gave power to the piezo-electric circuit of the accelerometer.
- the integrated D.C. voltage supply and signal amplifier which gave power to the strain gauge bridge of the load cell and amplified its output signal at a desired gain.

To impress on the shaker head a random or a sine wave motion, the output of either of the two signal generators, random noise or frequency generators, were fed through the Power Amplifier unit which drove the shaker.

Finally the output of the force and acceleration transducers were displayed either on the Frequency Analyser if the frequency content of the signal was of interest, or on the Oscilloscope for a time analysis of the signal.

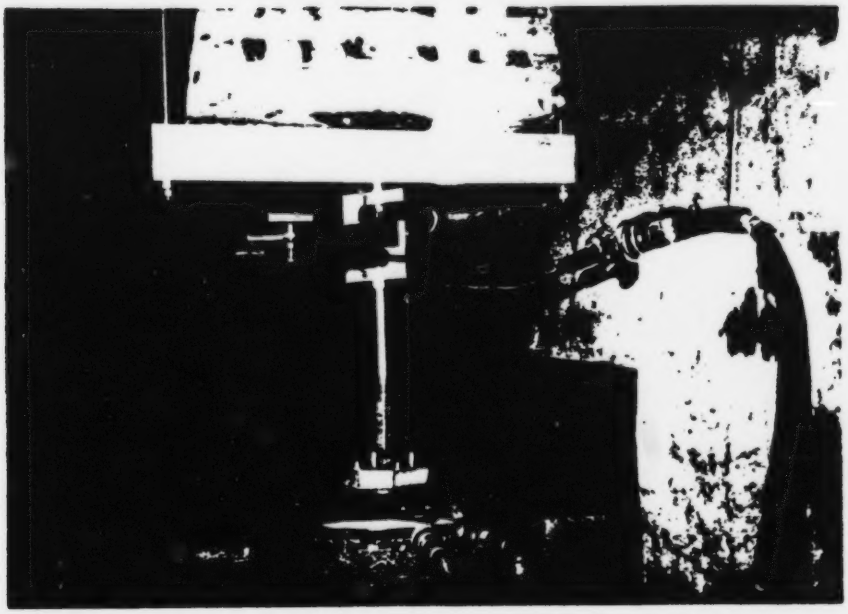

FIGURE NO. 5 ACCELEROMETER LOCATIONS ON TRACK TIE

FIGURE NO. 6 ACCELEROMETER LOCATIONS ON ST-49 SWITCH TIE

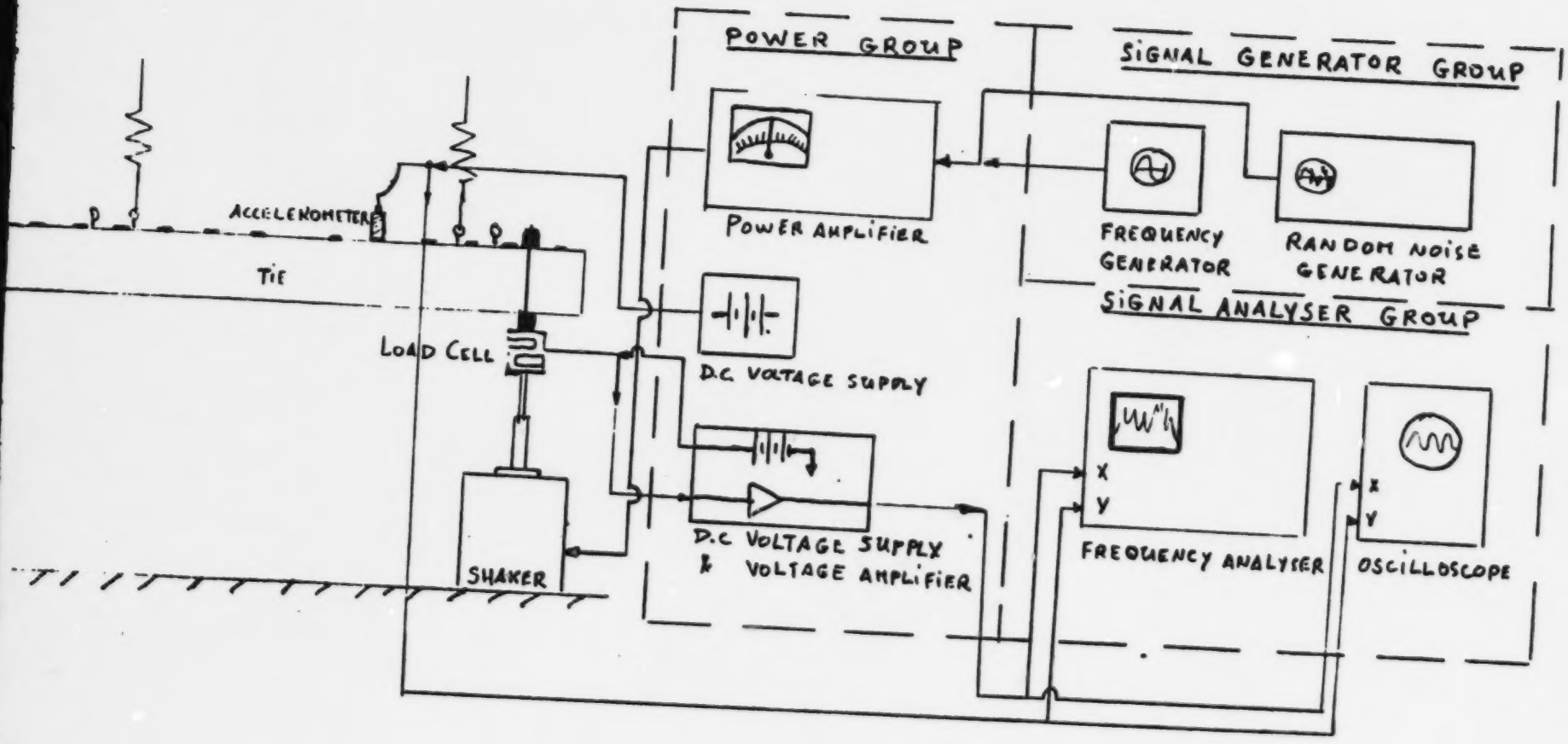

FIGURE NO. 7 INSTRUMENTATION LAYOUT

3. TEST PROCEDURE

This procedure was accomplished through the following six steps:

i) Installation of proper spring suspension system, between tie shoulders and crane hooks (see Figures Nos. 2 and 3).

ii) Link shaker to tie:

-raise tie off the supports

-position shaker and harness at a proper location along its length (see Figures Nos. 13 and 14 for better definition):

-for symmetrical modes position shaker at tie center (B,B')
-for asymmetrical modes position shaker at tie end (A,A')

-lower the tie, with its harness and load cell attached to it, at proximity to the top of the Quil-Shaker head assembly.

-level tie by activating either hoist

-link shaker to tie by screwing up nylon rod (Quil) into the bottom of the load cell.

iii) Take a wide band (0 to 1 KHz or 10 KHz) frequency response of the system in amplitude and phase using the Random Noise generator and the Spectrum analyses. This will give, quickly, an overall view of the resonant peaks and their frequencies.

iv) Zoom in on each peak respectively, by increasing the frequency resolution of the Frequency Analyser. Check to see if the coherence between the two signals (of load cell and accelerometer) is good. For each resonant mode, repeat this measurement with the accelerometer at different locations to get a spatial average of the dynamic characteristics over the tie length.

v) Repeat steps iii) and iv) with shaker positioned at other locations, so to avoid misinterpretations of phenomenon due to nodal point on the structure.

vi) To determine the mode shape at each of the resonant frequencies:

-set the sine wave generator to the resonant frequency.

-compare the signals of two accelerometers, one kept at a fixed location while the other is displaced on the aluminum blocks.

-from the 0° and 180° phase lag between the two traces on the oscilloscope, one can determine the relative amplitude (sign wise) between the thirteen locations, and henceforth the mode shape of the tie. At resonance any two points along a structure are either in phase or out of phase by 180 degrees.

Note: It is possible also to compare the outputs of accelerometer and load cell. They will present a +90° phase lag at resonance, between each station of the accelerometer.

4. MEASUREMENTS

4.1 Resonant Frequencies and Modes

Each resonant frequency is a global property of the structure and affects motion over the entire structure. The frequency characterizes a unique distribution of deformation across the structure (tie). This deformation is frequently referred to as mode shape. Through Spectral Analysis of the ratios of the acceleration signal (from accelerometer) to the force excitation signal (from the load cell), the resonant frequencies of the structure (or response function of the structure) can be found.

4.2 Frequency Spectra Interpretation

Resonance appears on the frequency spectra at peaks of relative amplitudes where the phase change is of 180° (or close to it) and for a high Coherence* value (85%).

The resonant frequencies of a structure are independent of the spatial location from which they are measured. But this does not apply to the magnitude of the resonant peaks. The sensor can be located at a nodal point of one of the higher resonant modes and therefore not detect or very weakly detect its resonance, due to the low amplitude of the resonant peak.

Hence there is a need to measure at different locations to obtain a clear picture of the resonant peaks (see Tables Nos. 6, 7 and 8 in Appendix No. 4 and Figures Nos. 9 to 11), they vary in amplitude depending on the location of the sensor and on the frequency bandwidth chosen. Therefore the phase response of the two signals is needed to certify whether or not it is a resonant peak.

The wide band frequency responses in amplitude and phase, were taken for the three ties tested. They are illustrated in Figures Nos. 15 to 17 (in Appendix No. 5).

Also Figures Nos. 18to 22 (in Appendix No. 5) illustrate focusing (ZOOM IN) on the individual resonant amplitude peaks, and they refer back to the wide band spectral response of CN60B tie (from Figure No. 16, in Appendix No. 5). These graphs show that the frequency response focused on each resonant peak produce a better definition in the peak. This enabled us to determine more precisely the resonant frequency and the half power frequencies needed to compute the structural damping coefficient at resonance.

Note, for higher frequencies, resonance is not as well characterized (see Figure No. 23, Appendix No. 5). More complex modes of vibration than flexure were introduced by the three dimensional nature of the structure.

* Coherence is the measure of the contamination of the two measured signals in terms of noise and non-linear effects.

4.3 Computation of Damping Coefficient

Basically, each resonance can be modelled by a second order spring, mass, damper system. This is possible under the assumption that the response of the structure is linear and that the damping is structural.

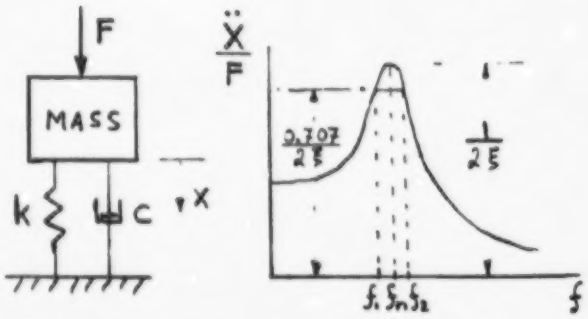

This statement is justified for broadly spaced resonant peaks and low damping coefficients (which is the case for the concrete ties).

An equivalent damping can be defined in terms of f_1, f_2, fn where f_1, and f_2 are the half power frequencies (at .707 of amplitude or -3dB) and where f_n is the resonnant frequency of the nth mode shape, such that it results in the structural damping coefficient

$$\eta_n = \frac{f_2 - f_1}{fn}$$

5. ANALYSIS OF TEST RESULTS

Data from Tables Nos. 6, 7 and 8 (Appendix No. 4) represent values measured at several locations on the structure for each resonant frequency. As they do not change very much as a function of location and should represent ideally a characteristic value at a given resonance, they were averaged out for each resonant mode.

These tables were condensed into Tables Nos. 1, 2 and 3.

Remarks:

-column three of Tables Nos. 6 to 8 (Appendix 4) represent the phase change between the two signals at each resonance. It should be close to 180° change.

-the shaker position on the ties tested were:

for CN60A Tie, at (A-A^1)

for CN60B Tie, at (B-B^1) for 101 Hz and 603 Hz
and at (A-A^1) for 310 Hz and 868 Hz

for (10 ft-6in.) Switch Tie at (A-A^1)

The locations (A-A^1) and (B-B^1) for each ties are shown on Figures Nos. 13 and 14.

5.1 Track Tie Data: CN60A, CN60B

i) Resonant Frequencies:

As shown in Tables Nos. 1 and 2 the first four resonant mode frequencies, of each of the two ties, are below 1KHz. Both ties have the same fundamental resonant frequency at 101 Hz. But for higher order modes of resonance the values of frequency diverge for the CN60A tie as compared to the CN60B tie, with lower values for the CN60B tie.

ii) Damping Coefficients:

The damping coefficients seemed relatively constant for the four resonant modes concerning the CN60A tie; whereas they varied for the CN60B tie, from one mode to the other.

There does not seem to be any noticeable pattern in the changes of the damping coefficient as a function of the modes. Measurement showed the highest damping coefficient to be at the first resonant mode for the CN60B with η - 1.8%.. In general the damping coefficients are of the same order of magnitude for both CN60A and CN60B ties, but they are not identical in value between the two ties tested at each mode. .

5.2 Turnout Tie Data

i) Resonant Frequencies:

As shown in Table No. 3, the first four resonant frequencies of the (10 ft-6 in.) Switch-Tie were all lower than those of the two track ties. Only the fundamental resonant frequency at 94 Hz was close to that of each track tie. These results were anticipated somewhat because of its greater length compared to the track ties.

It is important to realize that the (10 ft-6 in.) turnout tie tested is not representative of all the other ties in the turnout. They vary in length, from 9 ft. to 17 ft., to support the frog structure and the diverging tracks of the turnout.

Therefore a mathematical expression for frequencies was developed to apply to all the switch ties of different lengths (see Appendix No. 1). This frequency expression permitted the extrapolation of values of resonant frequencies for the Turnout ties of different lengths. A plot of these resonant frequencies versus tie length, for the first four modes, is plotted in Figure No. 8.

Note: The lines in Figure No. 8, characterizing each mode, should rather be discontinuous, because the length of the Switch ties are discrete values. A line was fitted through the points to underline the tendency of the frequency change with tie length. Other characteristics of this graph show that the resonant frequencies decrease as the tie lengths increase. Also the change in frequency is greater, as a function of the length, for the higher modes.

ii) Damping Coefficient

The coefficients are in a decreasing order as we go to the higher order modes. The highest damping coefficient is at 1.6% for the first resonant mode, which is similar in magnitude to that of the CN60B tie, at 1.8%.

Also, as a whole, the order of magnitude of the coefficient is the same as for the track ties CN60A and CN60B. Whether this coefficient changes as a function of tie length, at each mode of resonance, cannot be answered with certainty. Nevertheless it should be expected to be in the same order of magnitude, as we have seen between the two track ties and this Switch tie.

TABLE NO. 1

MODE CHARACTERISTICS OF CN60A TIE
(8'-3" Length)

Resonant Modes	Frequency (Hz)	Damping Average (%)	Mode Shapes
1st Symmetric	101.	0.6	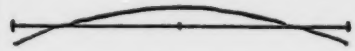
2nd Asymmetric	319.	0.6	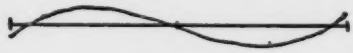
3rd Symmetric	638.	0.6	
4th Asymmetric	994.	0.5	

TABLE NO. 2

MODE CHARACTERISTICS OF CN60B TIE
(8'-3" Length)

Resonant Modes	Frequency (Hz)	Damping Average (%)	Mode Shapes
1st Symmetric	101	1.8	
2nd Asymmetric	310.	0.8	
3rd Symmetric	603.	0.6	
4th Asymmetric	868.	1.2	

TABLE NO. 3

MODE CHARACTERISTICS OF CN ST-49 TURNOUT TIE
(10'-6" Length)

Resonant Modes	Frequency (Hz)	Damping Average (%)	Mode Shapes
1st Symmetric	94.	1.6	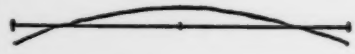
2nd Asymmetric	248.	1.0	
3rd Symmetric	466.	0.8	
4th Asymmetric	736.	0.6	

TABLE NO. 4

MODE CHARACTERISTICS OF CN BRIDGE TIE
Theoretical (12'-0" Length)

Resonant Modes	Frequency (Hz)	Damping Average (%)	Mode Shapes
1st Symmetric	86.	-	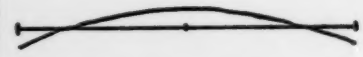
2nd Asymmetric	240.	-	
3rd Symmetric	472.	-	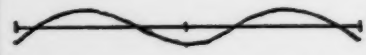
4th Asymmetric	781.	-	

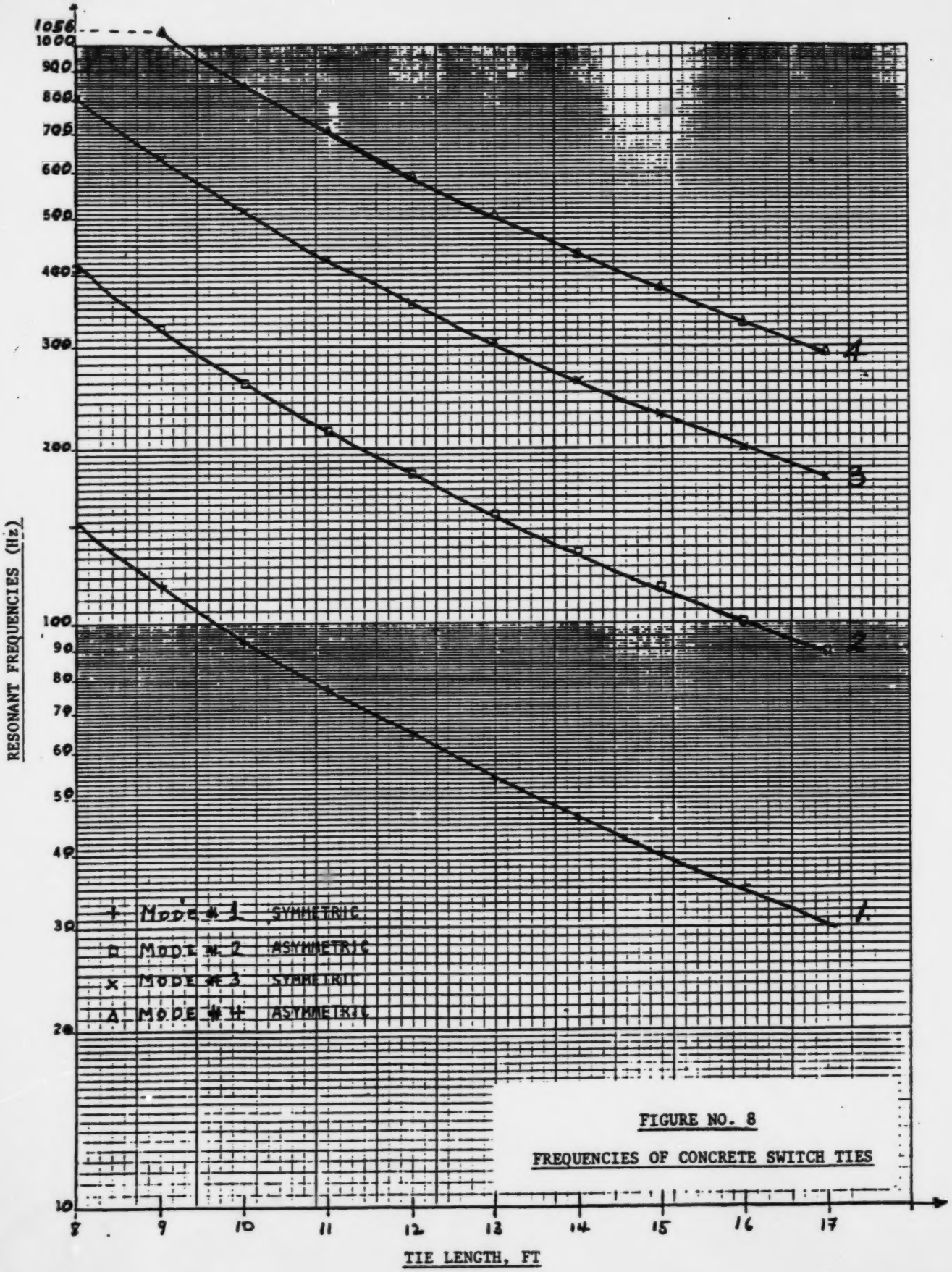

FIGURE NO. 8

FREQUENCIES OF CONCRETE SWITCH TIES

6. ANALYTICAL PREDICTION OF FREQUENCIES

The extrapolated values of frequencies for Switch ties of different lengths and for the Bridge ties were computed analytically through the use of Euler-Bernouilli beam equation (eq. 1).

$$\frac{\partial^4 y}{\partial x^4} + \frac{P}{EI}\frac{\partial^2 y}{\partial x^2} + \frac{m}{EI}\frac{\partial^2 y}{\partial t^2} = 0 \quad \text{(Eq. 1)}$$

and the analytical development of the beam frequency equation (Eq. 8 in Appendix No. 1).

The important factor which made this expression relevant in characterizing the tie frequencies was the elastic modulus of concrete Ec.

It had to be obtained by comparing the analytical frequencies pertaining to different elastic moduli to the measured frequencies of the CN No. 20 Turnout tie (see Table No. 5). The closest one of the sets of four frequencies to the test values would determine the appropriate coefficient of elastic modulus of the concrete. In the present use, results of column 5 Table No. 5, pertaining to the elastic modulus of concrete EC = 4.5 x 10^6psi, presented relative error values (% ER) in the average less than the other columns.

Note: The "% ER" as presented in Table No. 5, is the relative error of the calculated frequency with respect to the measured resonant frequency.

To have obtained analytically the values of frequency, it had been necessary to evaluate the moments of inertia of the composite cross-section of the Switch tie.

To calculate the moment of inertia, the area of the steel wire had to be transformed into an apparent concrete area. Also the neutral axis of the composite cross-section had to be computed prior to calculating the moment of inertia. In Appendix Nos. 2 and 3 a more detailed analytical development is presented with expression of neutral axis and of moments of inertia.

TABLE NO. 5

COMPARATIVE TABLE OF TEST AND PREDICTED FREQUENCIES

FOR (10 ft.-6 in) SWITCH TIE

$$F_{ANALYTICAL} = \frac{Al(n)}{2\pi} \cdot \sqrt{\frac{EI}{L^4 M}} \cdot \sqrt{Al(n)^2 + \frac{L^2 p}{EI}}$$

RESONANT MODES	TEST VALUES	ANALYTICAL VALUES				
		$E = 3 \times 10^6$ psi, $I = 827$ in.^{4}	$E = 4 \times 10^6$ psi, $I = 808$ in.^{4}	$E = 4.3 \times 10^6$ psi, $I = 805$ in.^{4}	$E = 4.5 \times 10^6$ psi, $I = 802$ in.^{4}	$E = 5 \times 10^6$ psi, $I = 797$ in.^{4}
#1	Al(1)	4.58	4.62	4.62	4.62	4.64
	F(Hz)	70.0	81.0	84.0	86.0	92.0
	% ER	+25%	+14%	+11%	+8%	+2%
#2	Al(2)	7.77	7.79	7.80	7.80	7.80
	F(Hz)	200.0	229.0	238.0	243.0	255.0
	% ER	+19%	+8%	+4%	+2%	-3%
#3	Al(3)	10.94	10.95	10.95	10.96	10.96
	F(Hz)	396.0	452.0	467.0	478.0	502.0
	% ER	+15%	+3%	2%	-2%	-8%
#4	Al(4)	14.10	14.10	14.11	14.11	14.11
	F(Hz)	656.0	748.0	775.0	792.0	832.0
	% ER	+11%	-2%	-5%	-8%	-13%
	-	-	-	-	-	-
	94.0	-	-	-	-	-
	-	-	-	-	-	-
	248.0	-	-	-	-	-
	-	-	-	-	-	-
	466.0	-	-	-	-	-
	-	-	-	-	-	-
	736.0	-	-	-	-	-
	-	-	-	-	-	-

Note:
- % ER = The relative error w.r.t. Test Values.
- Al(n) = The mode coefficient for nth mode.
- M = Mass per unit length.
- E = Modulus of Elasticity of Concrete.
- I = Moment of Inertia of Tie Section.
- L = Length.

7. THEORETICAL EVALUATION OF BRIDGE TIE FREQUENCIES

Having evaluated the elastic modulus of concrete (at $E_c = 4.5 \times 10^6$ lb./in.^{2}) based on the Switch Tie test results, the frequencies of the bridge tie were readily obtained. Here again the calculations of the neutral axis of the tie leading to those of the moment of inertia were run through. The moment of inertia was found to be $I = 1618$ in.^{4}. Then the parameter Al of the frequency expression (see equation 8 in Appendix 1) was obtained numerically by computer from the characteristic equation No. 7 in Appendix No. 1.

All these steps of calculations led to the frequencies shown in previous Table No. 4. They are quite similar to those of the CN No. 20 Turnout Tie. Unfortunately no damping coefficient were given, because there were no bridge ties available for testing.

8. DISCUSSION OF TEST RESULTS

8.1 Frequencies

As presented in Tables Nos. 1 to 4, the flexural resonant frequencies of ties vary from one to the other. They are function of four physical parameters presented in the frequency expression:

$$f = \frac{A^1(n)}{2\pi}\sqrt{\frac{gEI}{L^4W}} \cdot \sqrt{Al^2(n) + \frac{L^2P}{EI}}$$

which can usually be approximated by

$$f \simeq \frac{Al^2(n)}{2\pi}\sqrt{\frac{gEI}{L^4W}}$$

because $\frac{L^2P}{EI} << Al^2(n)$, in all practical consideration.

The four parameters are:

I	the moment of inertia of the cross-section
L	the length of the tie
W	the weight per unit length
Al(n)	the mode coefficient representative of the mode shape and axial loading

Changes in these four parameters will determine, for a given mode, any frequency variation. Little changes occur between frequencies of CN No. 20 Turnout tie and the Bridge tie as seen in Tables Nos. 3 and 4. This is due to the right variations between the four parameters of the two ties, but this is only a coincidence and would not necessarily be reproduced from the other Turnout ties.

8.2 Damping

Damping has been shown to vary as a function of the resonant frequency as seen in Tables Nos. 1 to 4.

Yet for a given mode of resonance, it should be representative of the mode shape of the tie, therefore constant along its length and not vary.

For a mode of resonance, any variations might be due to inaccuracies in the measurement technique due to localized changes in the strutural values. As a whole the structural damping measured inbending varies between .5 to 1.8% for these first four modes. These values are lower than the damping coefficient of 2.3% for a soft wood track tie measured at its first resonant mode of 102 Hz frequency. This was expected because wood is known for its good damping property. The wooden ties present an attenuated dynamic response compared to the concrete ties because of their higher structural damping coefficient measured in flexure. Also they dampen to a greater extent the vertical dynamic load, applied at the rail base because of their compressibility. So a force of lesser magnitude is transmitted to the rest of the tie.

The variation in structural damping, for the concrete ties, is in a given order of magnitude, as a whole. For a better basis of comparison in tie performances, it would be of value to establish a scheme by which one could compare the damping efficiency of a tie with more reliability.

The following are a few examples of schemes:

i) One could rely on damping on the first resonant mode. It has the advantage of being readily measured. Also it seems to be the highest of all the other modes, based on the present test results. One could take it as a reference representing the maximum level of damping for the rest of the resonant modes.

ii) One could avarage out the damping coefficient from the first few resonant mode values.

iii) One could reference the damping value to that of the most critical mode of resonance, as measured from track tests.

8.3 Theoretical Prediction

Unfortunately, as shown in Table No. 5, it is not an easy task to predict the exact values for the four resonant frequencies. One could only settle for a "closest fit" to the four measured frequencies. Column No. 5 in Table No. 5 was chosen as the most appropriate with an average error percentage of "0%". But as shown also, there can be as much as +8% error depending on the mode of resonance for that specific modulus of elasticity.

These discrepancies between theory and practice arise from the fact that Euler-Bernouilli equation models correctly the flexural response of a beam within the physical confines of a one-dimensional system (i.e. flexural wave lengths are much greater than the depth of the tie).

Otherwise for frequencies at which the dimensions of the section are of the same order of magnitude as the length of the propagating wave, this model fails to predict the higher mode vibratory nature of the tie.

It is stated by some authors* that to have not more than 10% error, the flexural wavelength should be greater than six times the depth of the beam.

* L. Cremer, "Structure-Borne Sound", Springer-Verlag 1973, p. 115.

Also these discrepancies might have come from the mass of the sensors and harness which could have changed the frequency response spectra of a structure by simply adding their own mass to the structure. Nonetheless the predicted frequencies for the concrete Bridge tie are good approximations. They might prove to be useful in relating resonant flexural modes of the tie to their resonant frequencies. And in general these measured or predicted values can be instrumental in pointing out vibrations from other modes than flexural (such as torsional) or from other structural members (such as bridge girders).

8.4 Comparison Between Analytical and Field Results

To illustrate bridge tie resonances on track, Figure No. 24, Appendix No. 5 represents the frequency spectra of the dynamic response of a bridge tie under the impact of a flat wheel of a loaded ballast car. Tie centre bending strains were registered. These results came from tests undertaken on a 29 foot girder bridge on the Drummondville Subdivision, in September 1984.

Two dominant crests can be distinguished, one at 88 Hz, the other at 468 Hz. They match quite closely the frequencies of the first and third resonant modes; this leads us to believe that the modes are present at these frequencies.

Also the sharp valley at 223 Hz, called a point of antiresonance, indicates here a nodal point in the tie vibration (a point of no motion). This frequency coincides with the predicted second resonant frequency at 240 Hz, again this seems to indicate the presence of the second resonant mode.

It is necessary to know the areas of the structure that undergo maximum motion in a particular mode, as these are the areas upon which corrective stiffness or mass terms will have maximum effect.

Figure No. 24 shows the usefulness of knowing the tie resonant frequencies in relating to the actual dynamic behaviour of the track.

9. GENERAL DISCUSSION

i) The frequency of passing wheels is much lower than that of any of the tie resonant frequencies. The ties will therefore not be forced into resonance, and they should not be subjected to destructive continuing vibrations.

Frequency of passing wheels on railway vehicles with 5.5 ft. axle spacing (minimum) relate to the following frequencies:

Speed		Frequency
fps	mph	cyc/sec (Hz)
5.5	3.75	1
55	37.5	10
110	75	20
220	150	40

ii) The concrete ties themselves have very low damping, but under the heavier axle loads, they are pressed tightly to the roadbed which has much higher damping capability.

iii) Regular track ties (CN60A and CN60B) will be deflected into their third mode shape (symmetric) under normal track loading conditions. Under impact loading from skid-flat wheels, which normally strike both rails at roughly the same time, the ties could be expected to be excited at their third mode resonant frequencies (638 Hz for the CN60A tie, 603 Hz for the CN60B tie). Under heavy pressure from loaded cars, the vibrations should be quickly damped by the ballast and roadbed.

iv) Under lightly loaded cars, the ties are not pressed as heavily into the ballast and damping will be less effective. There is an uplift wave on the rail under centers of cars (between the two trucks), and the ties may be lifted free of the damping ballast pressure. Under high speed lightly loaded vehicles, the impacted ties may set up a state of resonant vibration which is not damped out quickly by the roadbed. Sustained vibrations could be maintained. This has been measured and documented on British Rail where ties similar in design to the CN60A ties have been recorded ringing in flexure at roughly 640 Hz during the entire passage of trains. These resonant vibrations automatically imply reverse bending of ties, and the rail seat negative bending capacity of British ties has come under heavy scrutiny. Efforts are currently underway through Pandrol U.K. to attenuate some of these vibrations through use of improved rail/tie pads.

v) The CN bridge ties are supported by rubber pads on girders at 8 ft. spacing. The primary bending mode of the ties should therefore be the first, and there will be no damping from roadbed ballast. This will be documented in a future report covering strain gauge measurements on CN experimental bridge ties installed at mile 122.4 Drummondville Subdivision.

vi) The majority of the concrete turnout ties will be loaded asymmetrically on account of the divergence of tracks. The bending mode shapes that ties assume under traffic (including defective wheel impact loading) can only be determined through power spectral analysis of field measured data. This will be documented in a future report.

10. CONCLUSION

This report has documented most of the dynamic characteristics of the four types of concrete ties currently in service on CN Rail. At present, CN Rail Research has field measured high frequency (2000 Hz) bending strains on all four types of ties, under normal CN traffic conditions. More analysis will be done on all four sets of measurements.

CN installed a high speed (80 mph) concrete tie tangent test section on the Wainwright Subdivision in June of 1985, and Pandrol U.K. in concert with Genstar Costain Concrete Tie Co. Ltd. have taken high frequency concrete tie bending strain measurements. Ties were installed at both 24 and 26 in. spacings and the effects of tie pads ranging in thickness from 5 to 15 mm will be evaluated.

The frequencies, damping coefficients and mode shapes of the flexural resonant modes, documented in this report, will be useful:

i) in evaluating the performance of ties in track

ii) in understanding the track-tie behaviour through field measurements.

iii) in finding remedies to unwanted effects such as: destructive vibrations of track structure, reverse bending of ties and development of cracks.

iv) and finally in optimizing tie designs in view of reducing the production costs.

11. RECOMMENDATIONS

This report contains no recommendations because it has simply documented dynamic characteristics of concrete ties. It is to be hoped that the information contained herein will be useful in evaluating and predicting fatigue loading service lives of current and future concrete tie designs.

FIGURE NO. 9 DESCRIPTION OF CN60A CONCRETE TRACK TIE

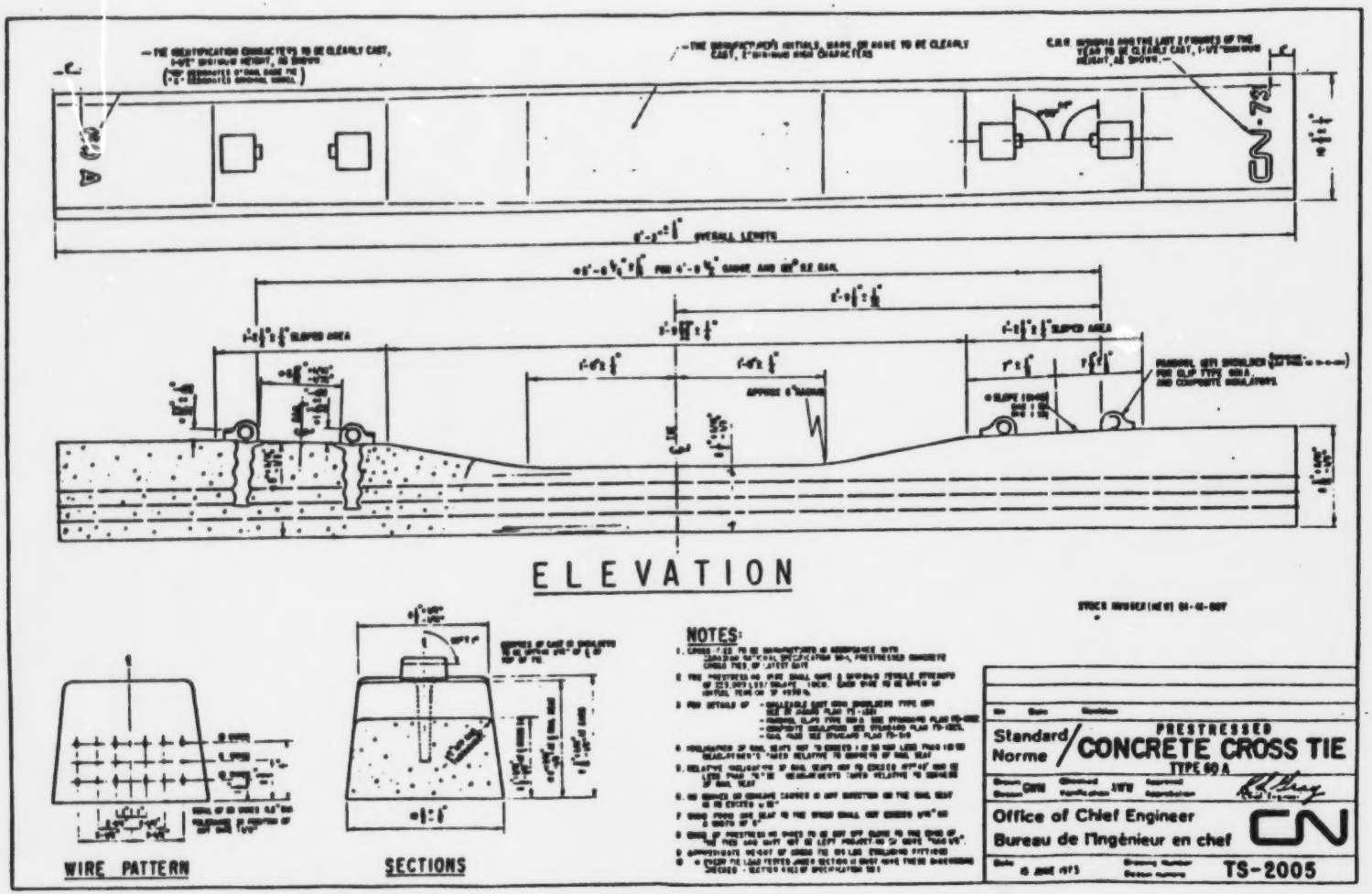

FIGURE NO. 10 DESCRIPTION OF CN60B CONCRETE TRACK TIE

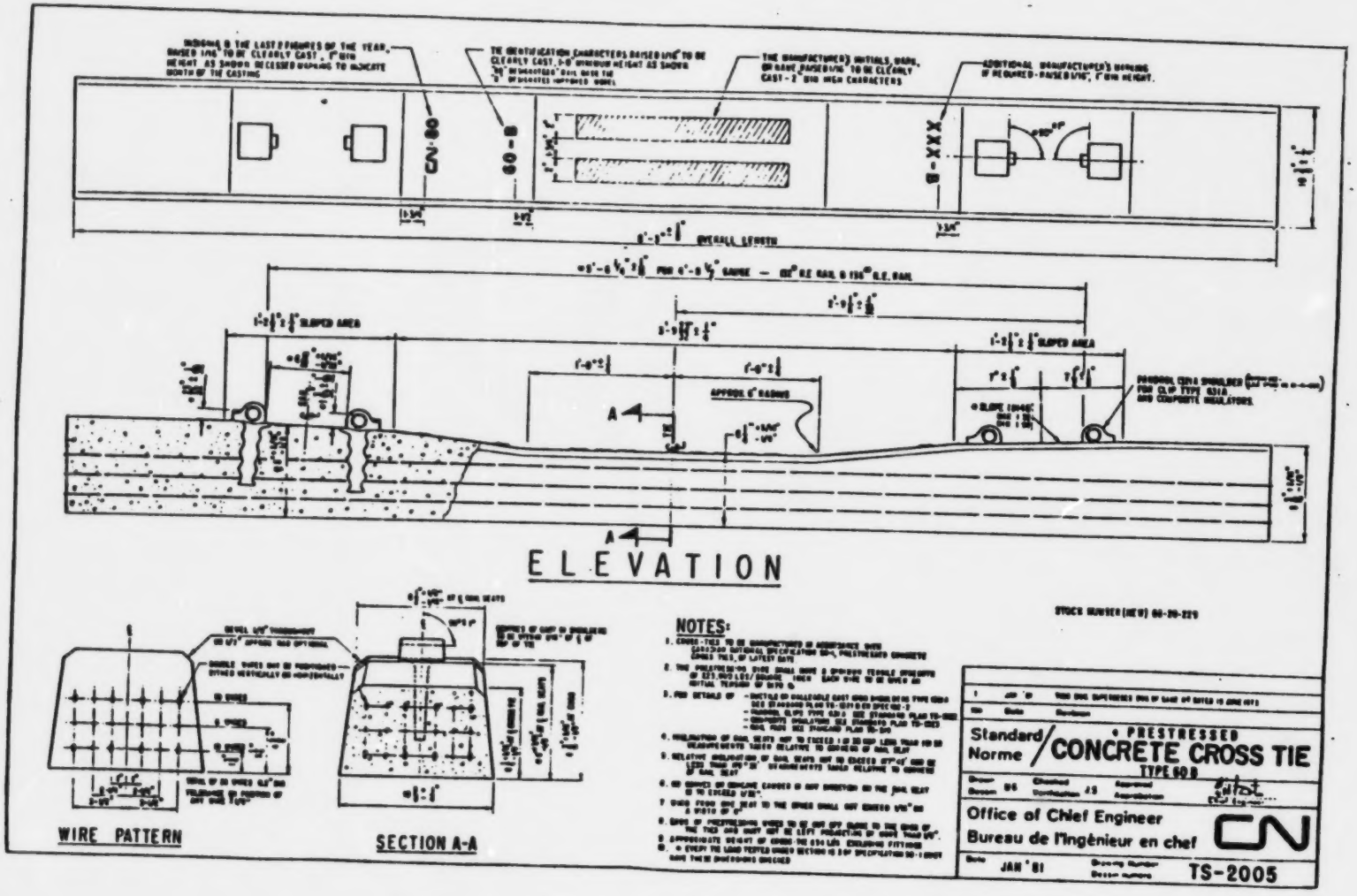

FIGURE NO. 11 DESCRIPTION OF CN CONCRETE TURNOUT TIES

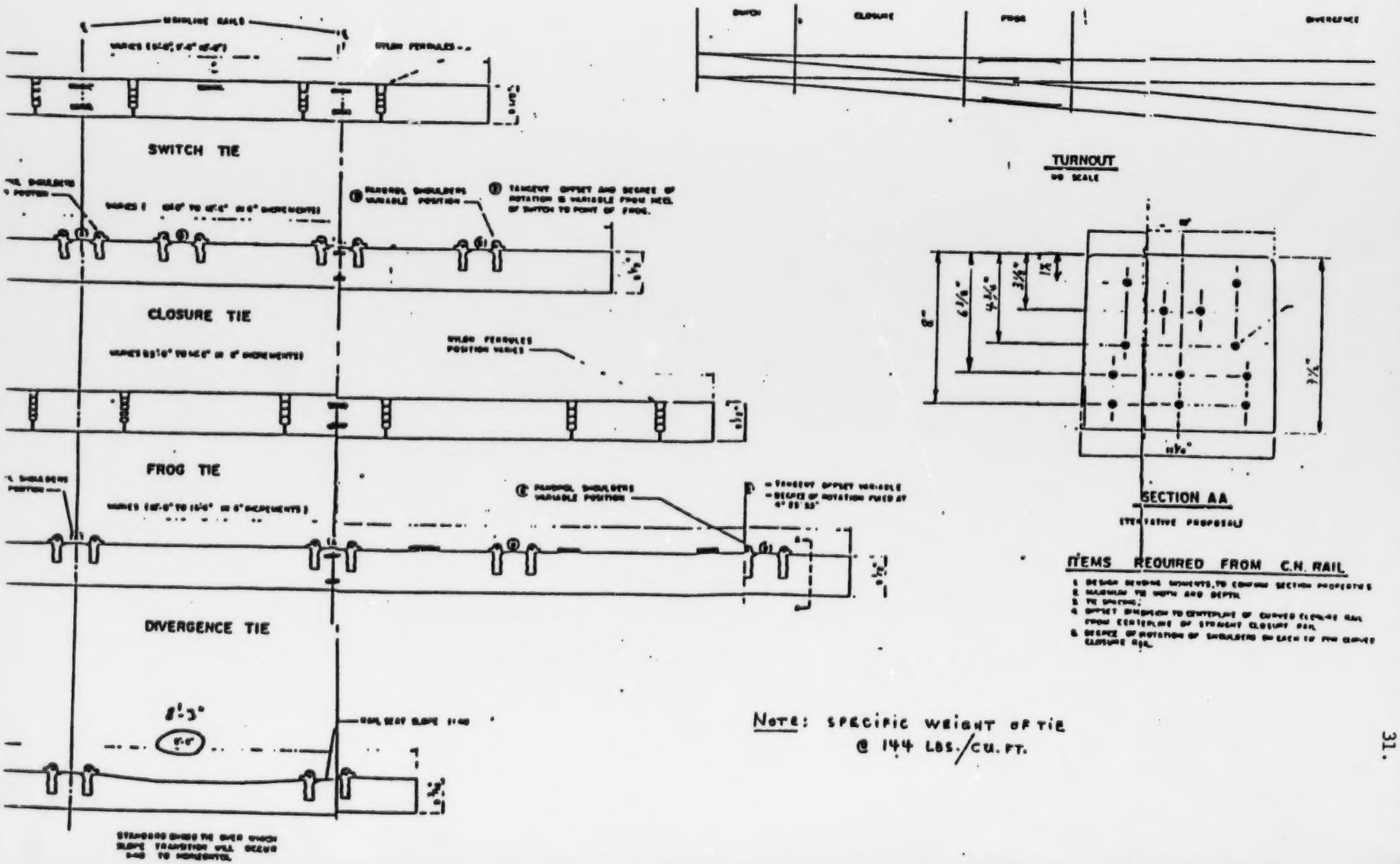

NOTE: SPECIFIC WEIGHT OF TIE @ 144 LBS./CU. FT.

FIGURE NO. 12 DESCRIPTION OF CN TYPE A CONCRETE BRIDGE TIE

(Drawing SK841 Dated 15 March 1984)

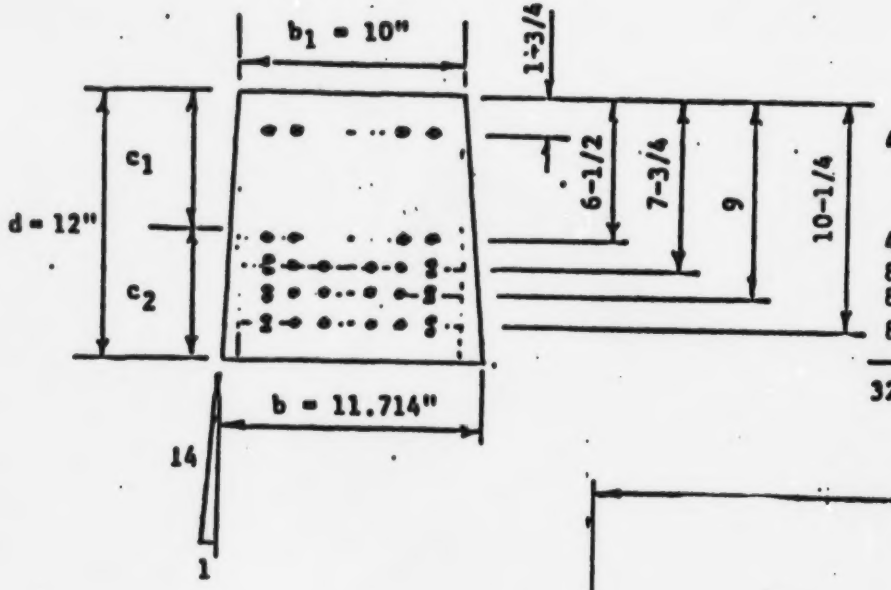

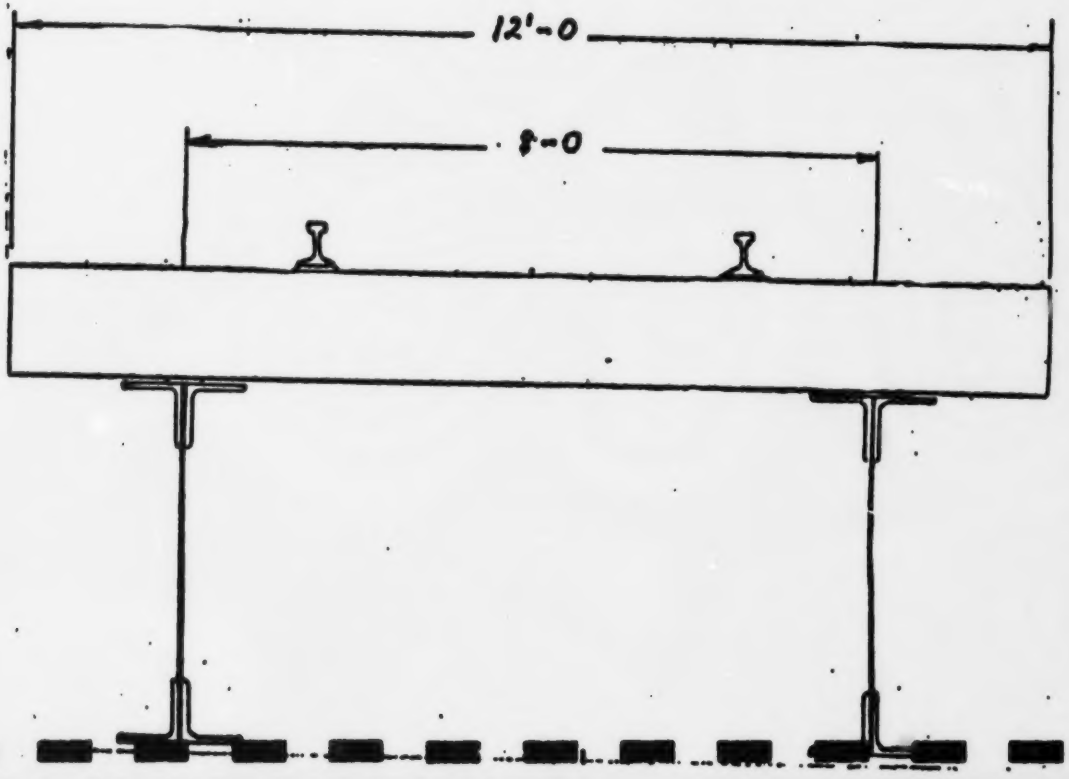

Tie Weight - 1563 lbs. with concrete @ 144 lbs./cu.ft.

FIGURE NO. 13 ACCELEROMETER STATIONS FOR CN60A & B TIES

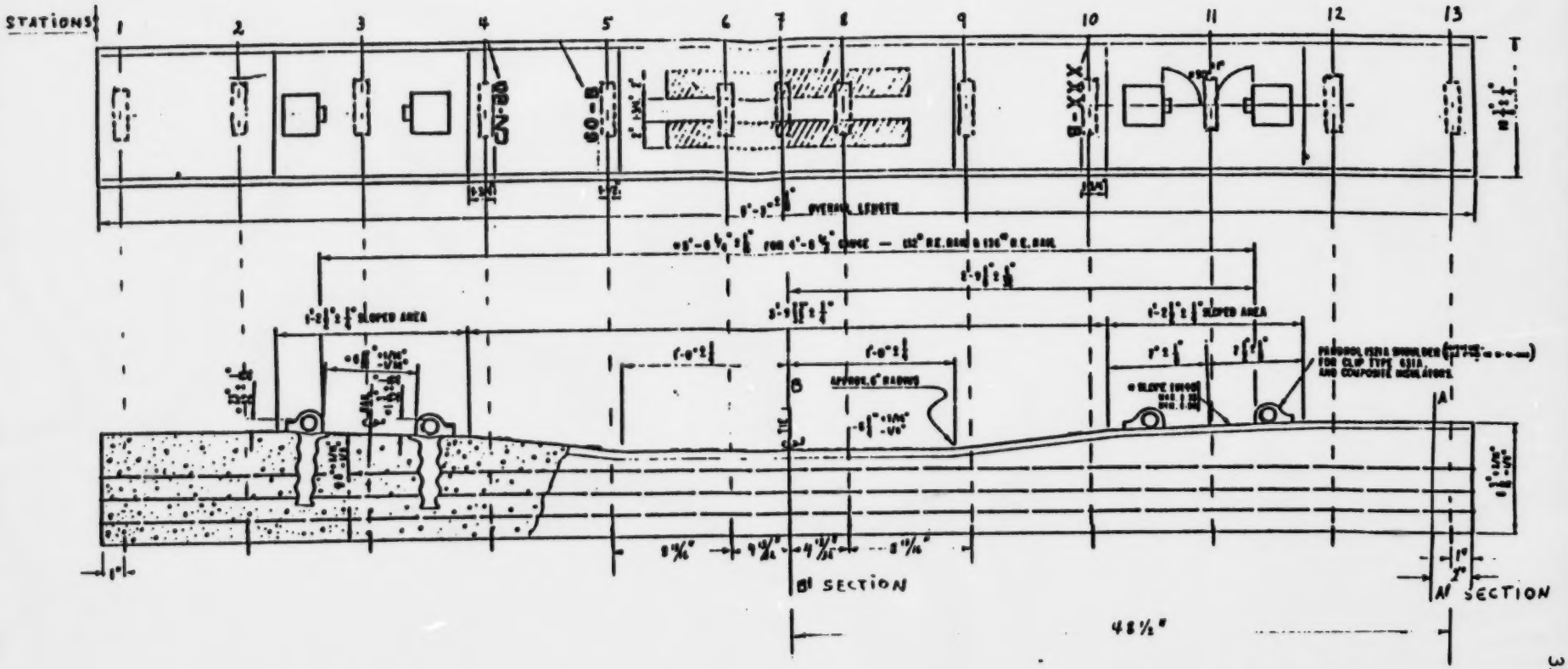

FIGURE NO. 14 ACCELEROMETER STATIONS FOR 10 ft. 6 in. SWITCH TIE

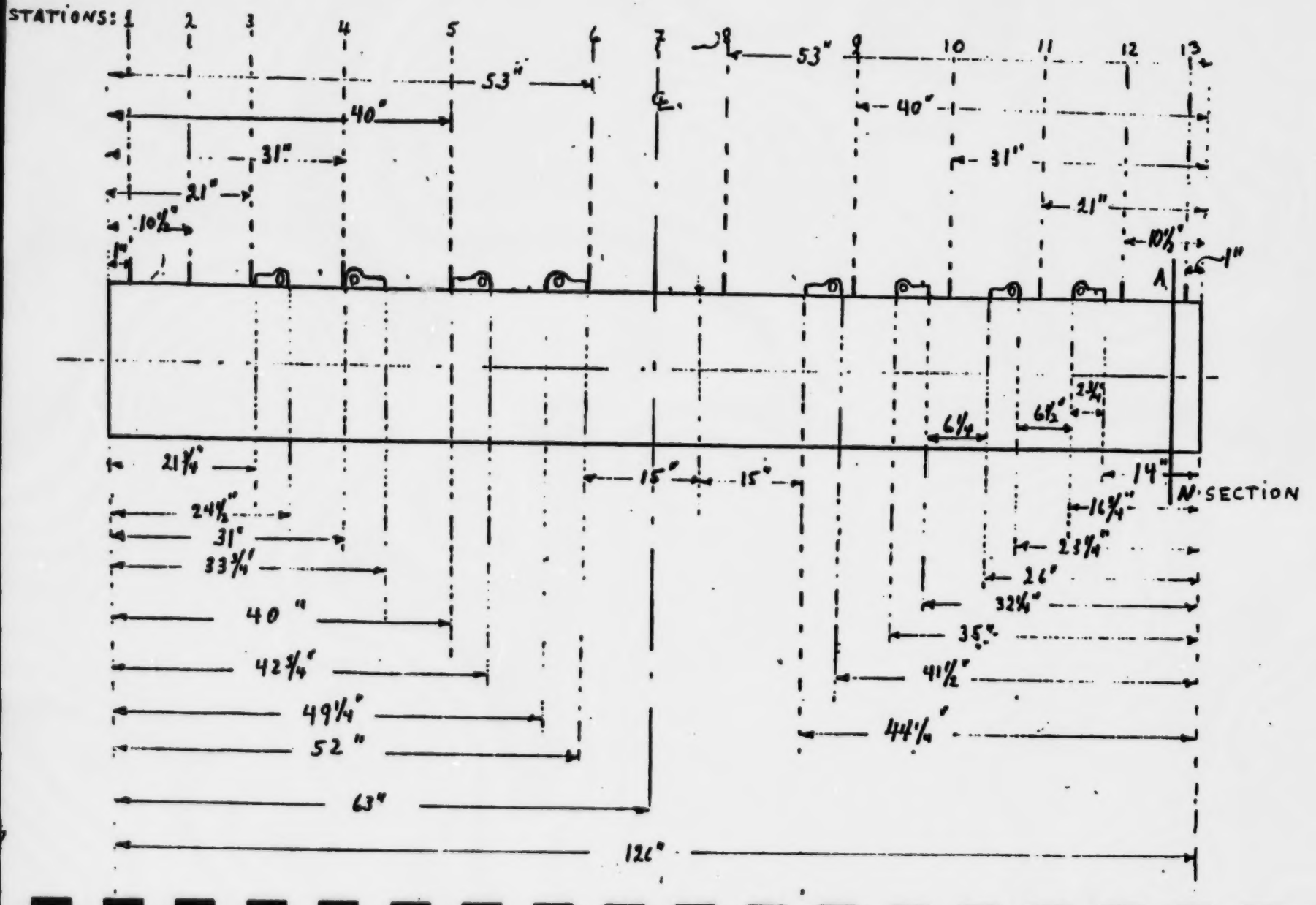

APPENDIX NO. 1

THEORETICAL EQUATIONS

APPENDIX NO. 1

Euler-Bernouilli's model of this system is:

$$\frac{\partial^4 y(x,t)}{\partial x^4} + \frac{P}{EI}\frac{\partial^2 y(x,t)}{\partial x^2} + \frac{m}{EI}\frac{\partial^2 y(x,t)}{\partial t^2} = 0 \qquad (1)$$

where: Y = lateral displacement of beam
P = 70% of prestress loading (final force in tie)
E = concrete elastic modulus
I = moment of inertia of cross-section
M = mass per unit length of tie

$Y(x,t) = V(x)\, e^{iwt}$, vertical displacement of tie for an harmonic motion. (2)

where: W = radial frequency

Substituting (2) in (1) gives:

$$\frac{d^4 V(x)}{dx^4} + K^2 \frac{d^2 V(x)}{dx^2} - B^4 V(x) = 0 \qquad (3)$$

where $K^2 = \frac{P}{EI}$, and $B^4 = \frac{MW^2}{EI}$

Then non-dimensionalizing equation (3) for practical purposes, setting: $\bar{x} = \frac{x}{L}$, $\bar{V} = \frac{V}{L}$, $K = KL$, $\bar{B} = BL$

Substituting these values in (3) gives:

$$\bar{V}''''(\bar{x}) + \bar{K}^2 \bar{V}''(\bar{x}) - \bar{B}^4 \bar{V}(\bar{x}) = 0 \qquad (4)$$

Factoring out $\bar{V}(\bar{x})$ in (4) renders the exponential coefficients in the generalized expression of $\bar{V}(\bar{x})$.

$$(D^4 + \bar{K}^2 D^2 - \bar{B}^4)\, V(\bar{x}) = 0 \qquad (5)$$

APPENDIX NO. 1

Equation No. 5 leads to the exponential coefficients A1 and iA2:

$$A1^2 = -\frac{\bar{K}^2}{2} + \sqrt{\frac{\bar{K}^4}{4} + \bar{B}^4}$$

$$i^2 A2^2 = i^2\left(\frac{\bar{K}^2}{2} + \sqrt{\frac{\bar{K}^4}{4} + \bar{B}^4}\right) \qquad (6)$$

which results in the expression of $\bar{V}(\bar{x})$:

$$\bar{V}(\bar{x}) = A \cosh A1.\ \bar{x} + B \sinh A1.\ \bar{x} + C \cos A2.\ \bar{x} + D \sin A2.\bar{x}$$

For boundary conditions of a Free-Free beam

where: $\dfrac{\partial^2 \bar{V}(\bar{x})}{\partial \bar{x}^2} = 0$ and $\dfrac{\partial^3 \bar{V}(\bar{n})}{\partial \bar{x}^3} = 0$; for $\bar{x} = 0, 1$

one ends up with the "characteristic equation":

$$2.\ (1 - \cosh A1\ .\ \cos A2) + \sinh A1, \sin A2\ .\ \frac{\bar{K}^2(\bar{K}^4 + 3\ A1^2 A2^2)}{(A1^3, A2^3)} = 0 \qquad (7)$$

Knowing that $A1^2 = A2^2 - \bar{K}^2$, equation (7) is expressed only in terms of coefficient A1. This value (or mode coefficient) relates the frequency to the mode of resonance.

Then rewriting (Eq. 6), with the frequency in terms of the mode coefficient A1(n) for the nth mode, one obtains:

$$F(n) = \frac{A1(n)}{2n}\ .\ \frac{EI}{L^4 M}\ .\ \sqrt{A1(n)^2 + \bar{K}^2} \qquad (8)$$

where the n^{th} nodal frequency F(n) is resolved from the value of A1(n) determined by equation (7).

APPENDIX NO. 2

TIE CENTROID LOCATION

APPENDIX NO. 2

CENTROID LOCATION

It is important to locate the depth of the centroid for the composite beam section, if one wants to be able to calculate the moment of inertia.

Due to the fact that all the area of concrete is in a compressive prestress, this hole section strains linearly about this centroid either in tension or compression, in the limits of elasticity of the concrete prestress.

Therefore one must find the location of the centroid of the areas composed of concrete and of steel. The steel areas have to be transformed into their equivalent concrete sections: $n = \frac{ES}{Ec}$

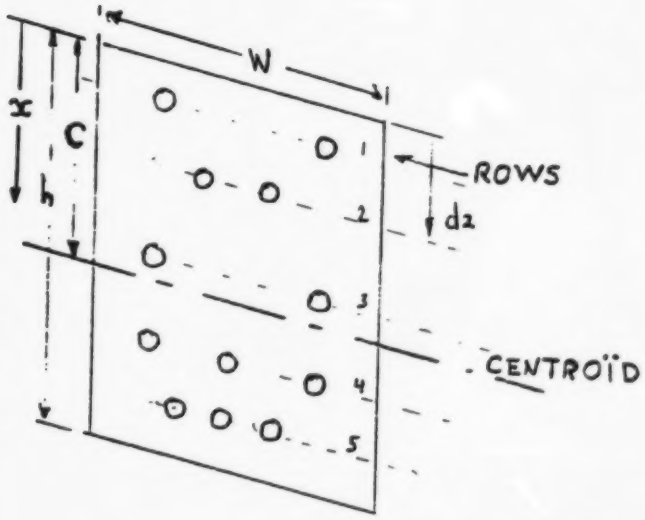

Based on theory $\Sigma F = 0$, over the cross-section,

$$\Sigma F = \int_A \sigma \, dA = 0 \Rightarrow \int_A W \frac{Mx}{I} \, dx = 0$$

$$\Rightarrow \int_A W \, x dx = 0$$

$$\Rightarrow \Sigma \; Ai.\bar{x}i = 0 \qquad (1)$$

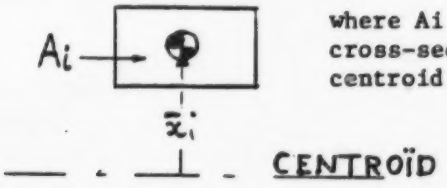

where Ai are the different areas of the cross-section and xi the distance of its centroid to a datum line.

Note: An important step in computing the centroid, is to assume initially its relative position on the cross-section.

APPENDIX NO. 2

Definition of different parameters:

As = area of steel wire

ri = no. of wires per row, where i = 1, 2,...., b

b = total no. of rows of wire

di = distance from top of tie to i^{th} row

t = no. of rows above centroid

c = depth of centroid from top of tie

The equation to resolve the locaation of the centroid based on expression (1) is expressed as:

$$W \frac{c^2}{2} + \sum_{i=1}^{t} ri.As(n-1)\cdot(c-di)$$

$$= W \frac{(h-c)^2}{2} + \sum_{i=t+1}^{b} ri \cdot As(n-1).(di-c)$$

APPENDIX NO. 3

TIE MOMENT OF INERTIA

APPENDIX NO. 3

TIE MOMENT OF INERTIA

Because the composite cross-section of the ties are in a prestressed state, all the section (concrete and steel) strains uniformly about the new Neutral axis, within the limits of the prestress distribution over the section. Therefore in calculating the new moment of inertia for the "effective flexural rigidity" EI, the transformed cross-sectional area had to be considered.

And the calculations were done with reference to the new Neutral axis pertaining to the transformed cross-section.

In the case of the Switch Tie, the transformed area would look like this:

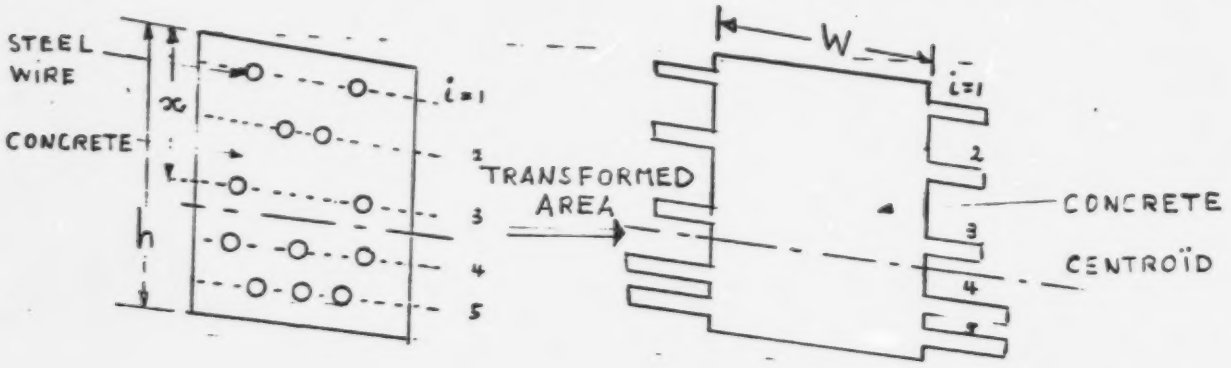

This new moment of inertia comes out from considerations of the "effective flexural rigidity" EI defined as such:

$$EI = Ec\ Ic + Es\ Is$$

where subscripts c and s relate the values to concrete and steel respectively.

APPENDIX NO. 3

MOMENT OF INERTIA

Transforming all the cross-section into apparent concrete area and assuming the modulus of concrete is known Ec, then the new moment of inertia I^1 follows:

$$EI = Ec.Ic + Es.Is$$

$$= Ec.(Ic + (Es/Ec).Is)$$

$$= Ec \cdot I^1$$

Using the "Parallell Axis" formulas:

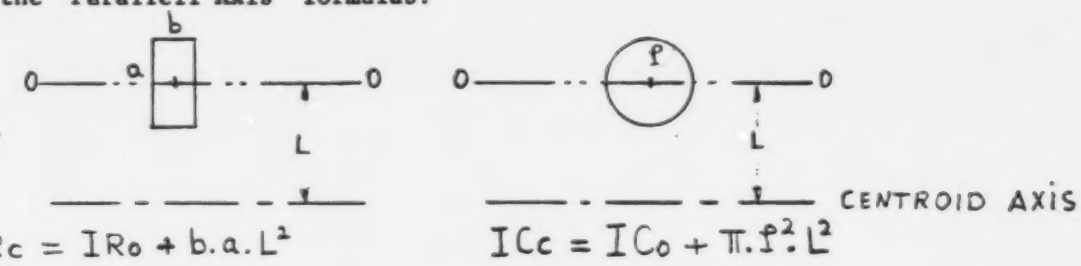

and relating to the tie cross-section, we develop

$$IB_c = \frac{Wh^3}{12} + Wh(x - h/2)^2$$

IC_o (moment of inertia of wire) $= \frac{\pi f^4}{4}$

So expanding I^1 we get the following expression:

$$I^1 = \frac{Wh^3}{12} + Wh(x - h/2)^2$$

$$+ \sum_{i=1}^{t} \left(ri.\frac{\pi f^4}{4} + ri.\pi f^2(n-1).(x-di)^2 \right)$$

$$+ \sum_{i=t+1}^{b} \left(ri.\frac{\pi f^4}{4} + ri.\pi f^2(n-1).(di-x)^2 \right)$$

APPENDIX NO. 4

DYNAMIC TEST DATA FOR

CN60A, CN60B, CN NO. 20 TURNOUT TIES

TABLE NO. 6

DYNAMIC TEST DATA FOR CN60A TIE

Station No.	Resonant Freq. (Hz)	Phase Angle (°)	1/2 Power Frequencies F1 (Hz)	F2 (Hz)	Damping Coeff. (%)
11	101.	180°	100.5	101.1	0.3
7	101.	180°	100.4	101.1	0.3
1	101.	180°	100.4	101.1	0.3
11	319.	180°	318.5	320.4	0.3
7	319.	180°	318.2	320.2	0.3
1	319.	180°	318.4	320.1	0.3
11	638.	180°	635.6	639.2	0.3
7	638.	160°	635.6	638.8	0.3
1	637.	180°	636.4	638.8	0.2
11	994.	180°	991.9	997.0	0.3
7	994.	180°	991.9	996.3	0.2

TABLE NO. 7

DYNAMIC TEST DATA FOR CN60B TIE

Station No.	Resonant Freq. (Hz)	Phase Angle (°)	1/2 Power Frequencies F1 (Hz)	F2 (Hz)	Damping Coeff. (%)
1	101.	180°	100.1	101.7	0.8
2	101.	180°	100.0	102.1	1.0
6	101.	180°	100.0	102.1	1.0
5	101.	180°	100.0	102.1	1.0
7	101.	180°	100.3	101.9	0.8
1	310.	180°	308.9	311.5	0.4
2	310.	180°	308.7	311.3	0.4
3	310.	180°	308.5	311.4	0.5
11	310.	180°	308.8	311.5	0.4
12	310.	180°	308.7	311.6	0.5
1	603.	165°	601.1	604.9	0.3
2	603.	162°	601.0	605.1	0.3
5	603.	162°	601.0	604.8	0.3
6	603.	162°	601.0	604.9	0.3
7	603.	168°	601.0	605.0	0.3
5	869.	180°	862.6	872.8	0.6
9	867.	180°	862.5	872.1	0.6

TABLE NO. 8

DYNAMIC TEST DATA FOR CN CONCRETE SWITCH TIE

Station No.	Resonant Reson.(Hz)	Phase (°)	1/2 Power Frequencies F1 (Hz)	F2 (Hz)	Damping Coeff. (%)
7	94.	-	-	-	0.8
5	248.	180°	246.4	249.0	0.5
9	248.	180°	246.4	249.1	0.5
11	248.	180°	246.6	249.1	0.5
12	248.	180°	246.7	248.8	0.4
5	466.	180°	464.1	467.4	0.4
9	466.	180°	464.4	467.6	0.3
11	466.	180°	463.9	467.8	0.4
12	466.	180°	463.8	467.5	0.4
5	736.	180°	733.8	738.9	0.3
9	736.	170°	733.8	738.7	0.3
11	737.	180°	733.9	739.0	0.3
12	737.	180°	733.8	739.4	0.4

APPENDIX NO. 5

FREQUENCY RESPONSE PLOTS OF

CN60A, CN60B, CN NO. 20 TURNOUT TIES

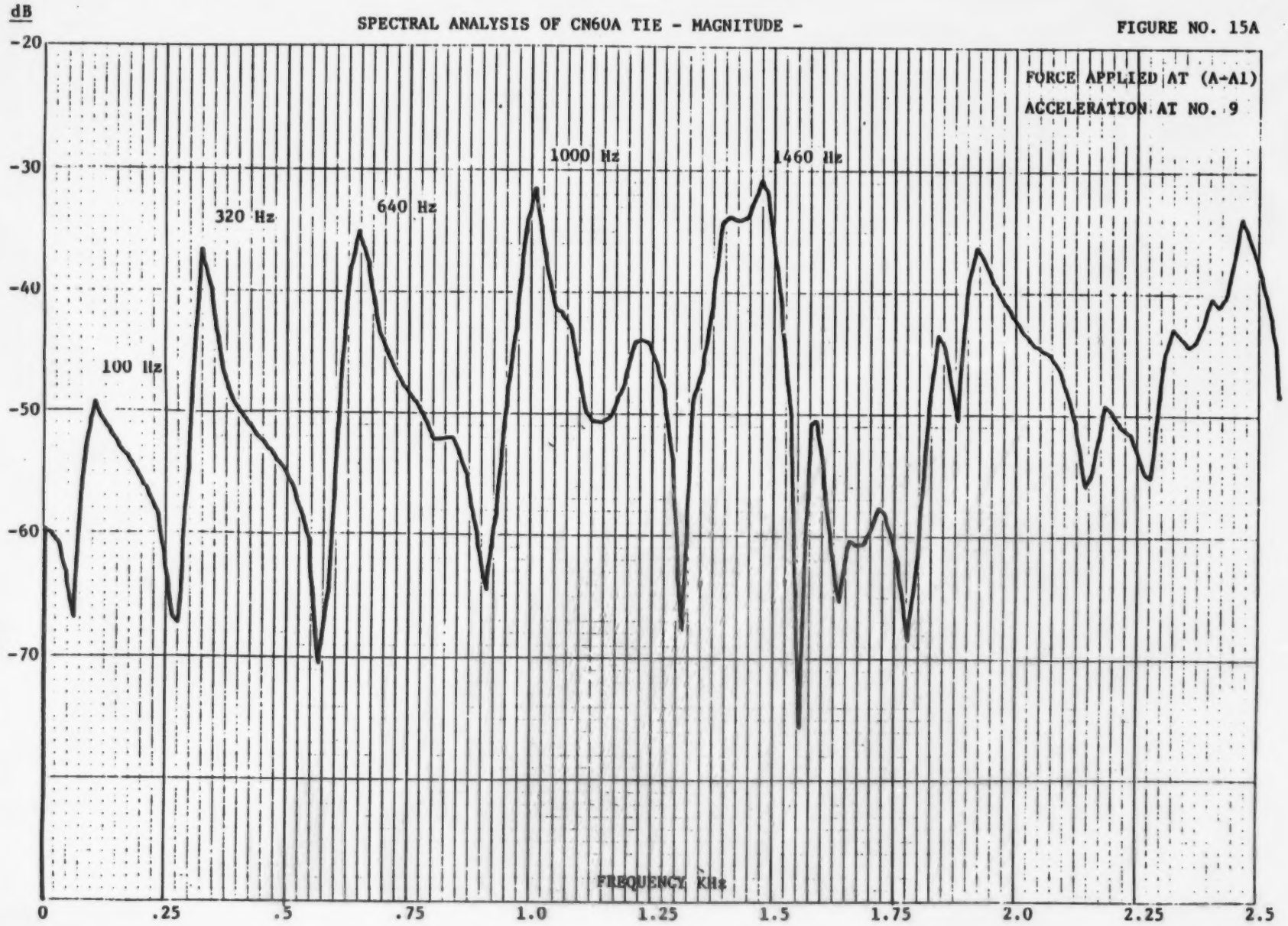
dB
SPECTRAL ANALYSIS OF CN60A TIE - MAGNITUDE -
FIGURE NO. 15A
FORCE APPLIED AT (A-A1)
ACCELERATION AT NO. 9
-20
-30
-40
-50
-60
-70
100 Hz
320 Hz
640 Hz
1000 Hz
1460 Hz
FREQUENCY KHz
0
.25
.5
.75
1.0
1.25
1.5
1.75
2.0
2.25
2.5

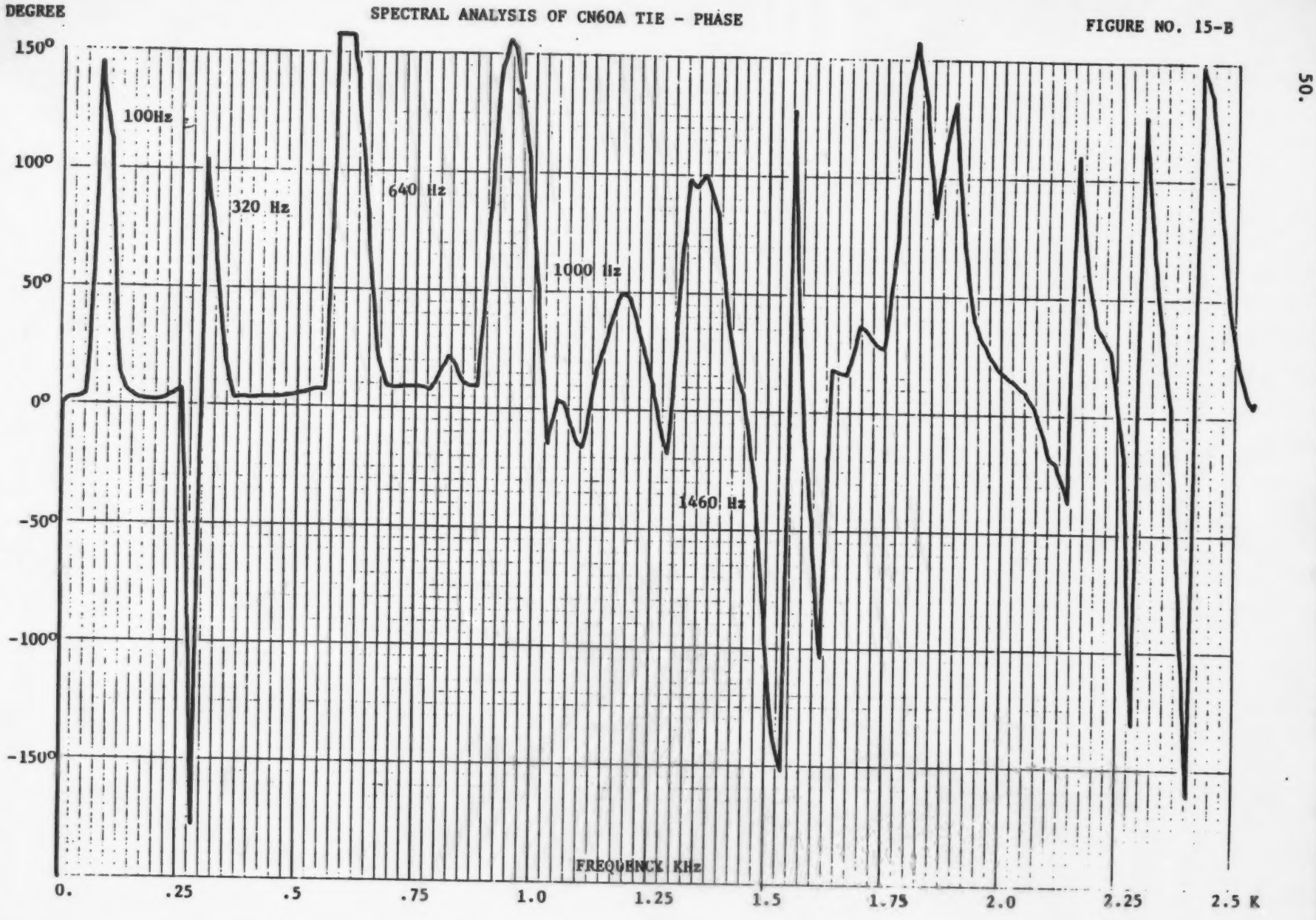
DEGREE
SPECTRAL ANALYSIS OF CN60A TIE - PHASE
FIGURE NO. 15-B
150°
100°
50°
0°
-50°
-100°
-150°
100Hz
320 Hz
640 Hz
1000 Hz
1460 Hz
FREQUENCY KHz
0.
.25
.5
.75
1.0
1.25
1.5
1.75
2.0
2.25
2.5 K

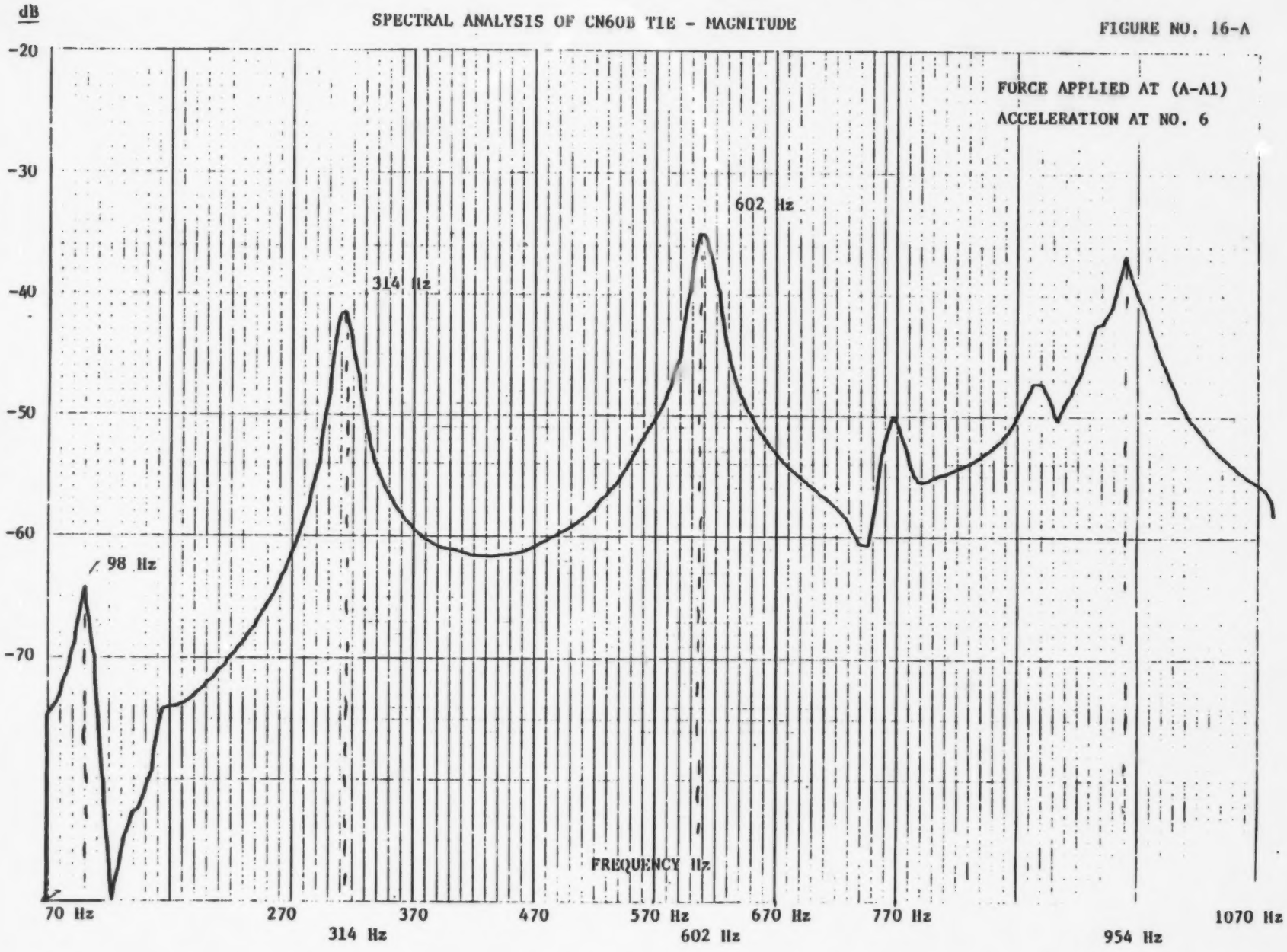
dB
SPECTRAL ANALYSIS OF CN60B TIE - MAGNITUDE
FIGURE NO. 16-A
FORCE APPLIED AT (A-A1)
ACCELERATION AT NO. 6
-20
-30
-40
-50
-60
-70
602 Hz
314 Hz
98 Hz
FREQUENCY Hz
70 Hz
270
370
470
570 Hz
670 Hz
770 Hz
1070 Hz
314 Hz
602 Hz
954 Hz

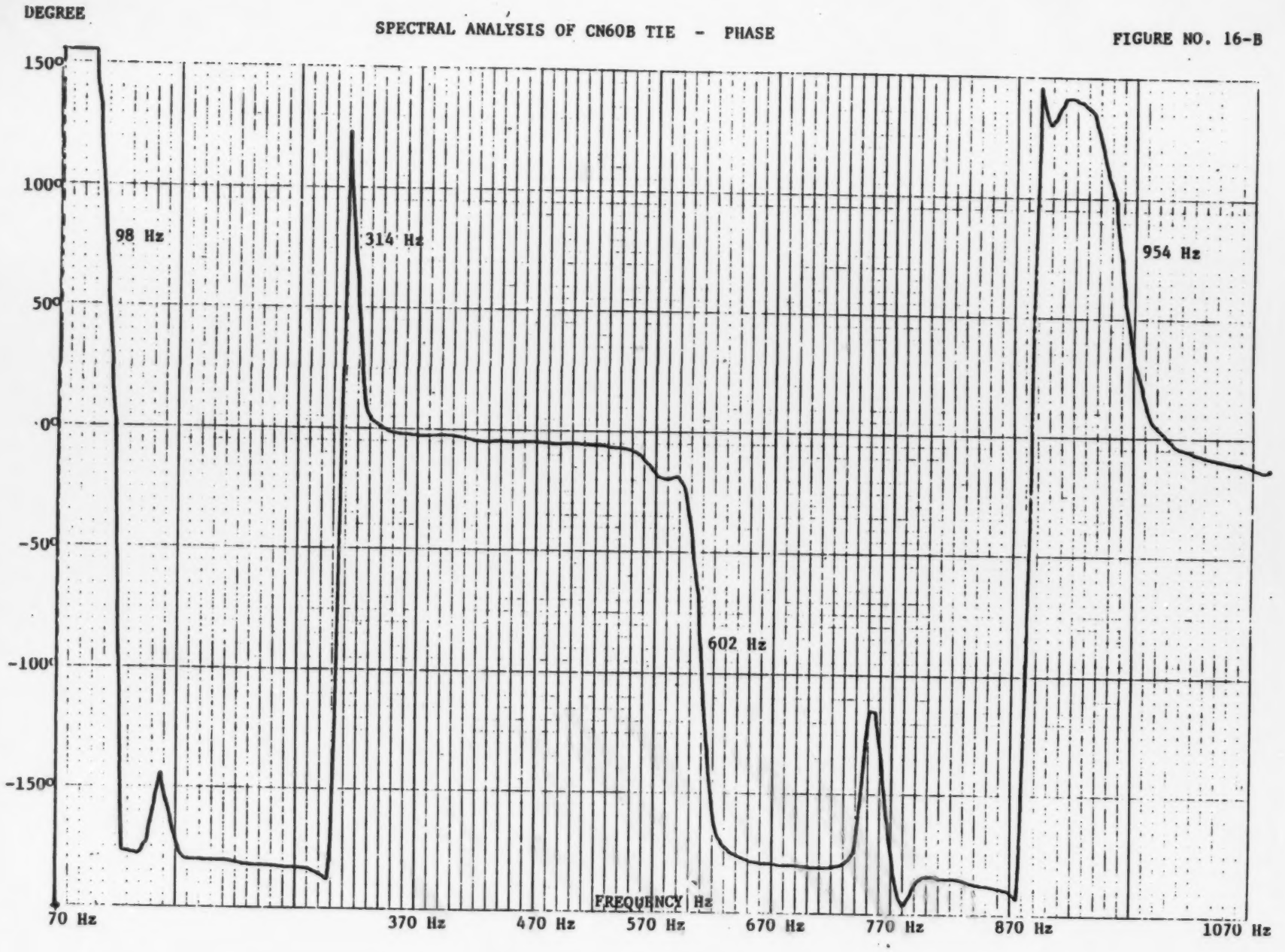
DEGREE
SPECTRAL ANALYSIS OF CN60B TIE - PHASE
FIGURE NO. 16-B
1500
1000
500
0°
-500
-1000
-1500
98 Hz
314 Hz
602 Hz
954 Hz
FREQUENCY Hz
70 Hz
370 Hz
470 Hz
570 Hz
670 Hz
770 Hz
870 Hz
1070 Hz

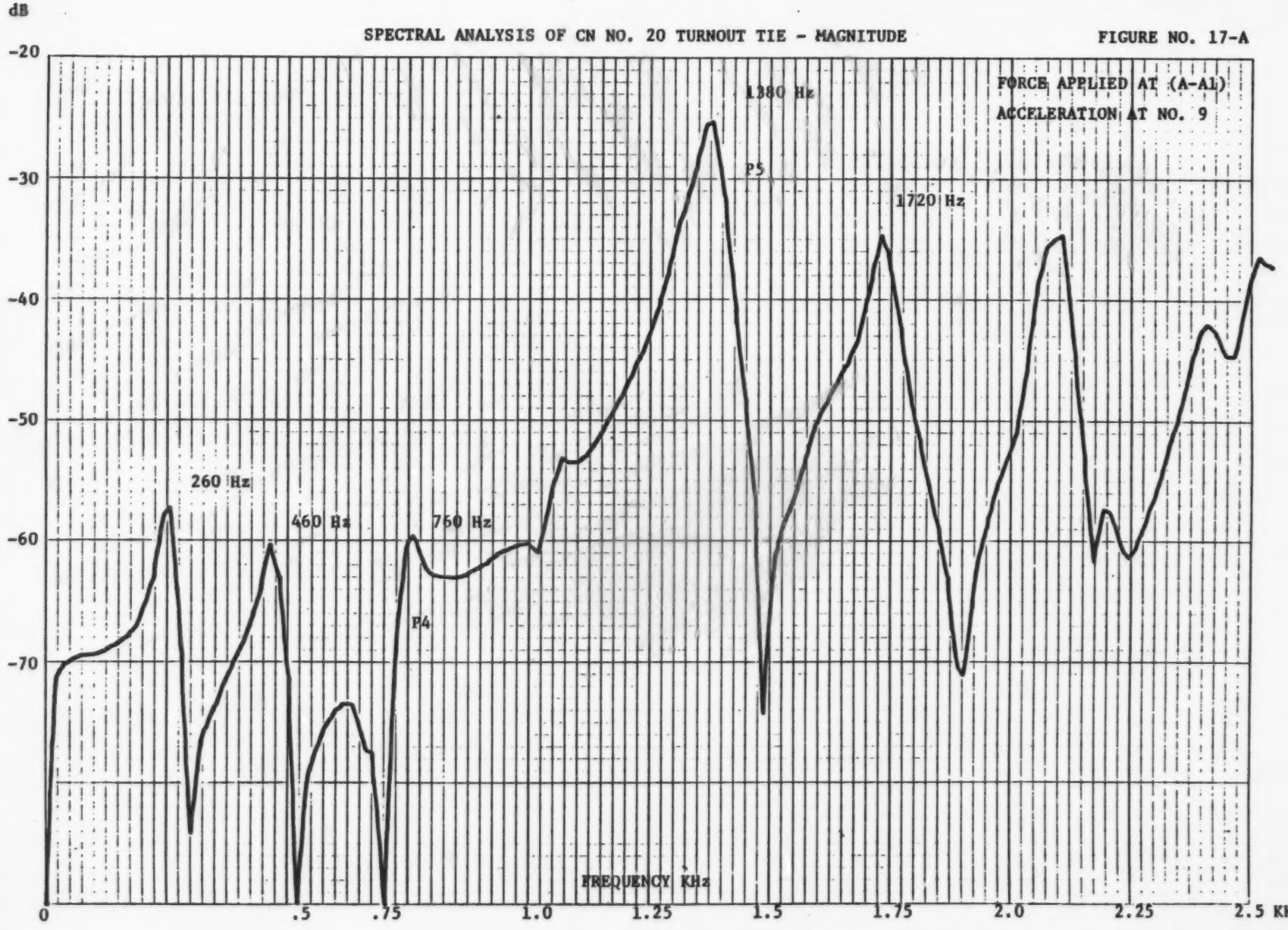
dB
SPECTRAL ANALYSIS OF CN NO. 20 TURNOUT TIE - MAGNITUDE
FIGURE NO. 17-A
FORCE APPLIED AT (A-A1)
ACCELERATION AT NO. 9
-20
-30
-40
-50
-60
-70
1380 Hz
P5
1720 Hz
260 Hz
460 Hz
760 Hz
P4
FREQUENCY KHz
0
.5
.75
1.0
1.25
1.5
1.75
2.0
2.25
2.5 KHz

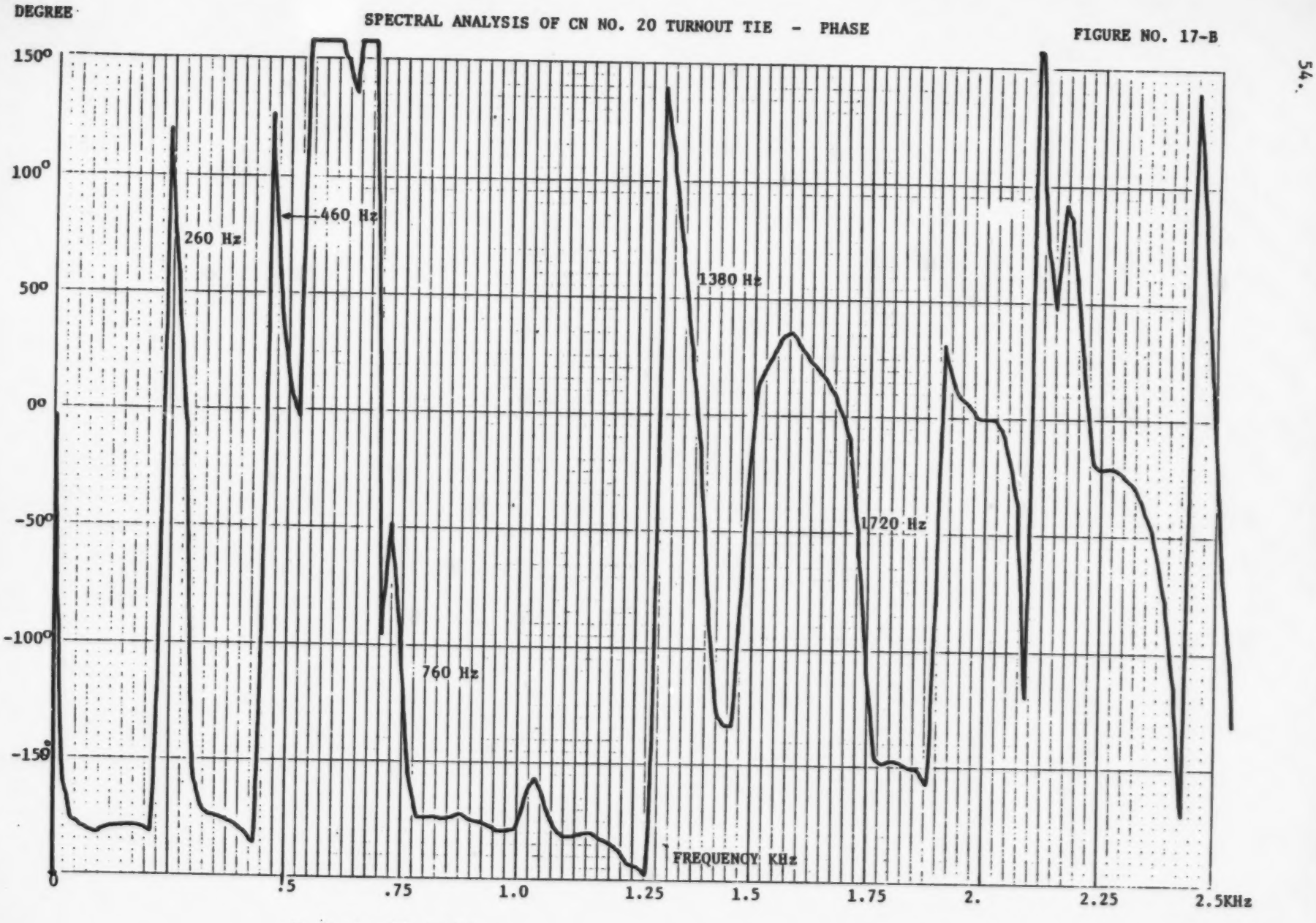
DEGREE
SPECTRAL ANALYSIS OF CN NO. 20 TURNOUT TIE - PHASE
FIGURE NO. 17-B
150°
100°
50°
0°
-50°
-100°
-150°
260 Hz
460 Hz
760 Hz
1380 Hz
1720 Hz
0
.5
.75
1.0
1.25
1.5
1.75
2.
2.25
2.5KHz
FREQUENCY KHz

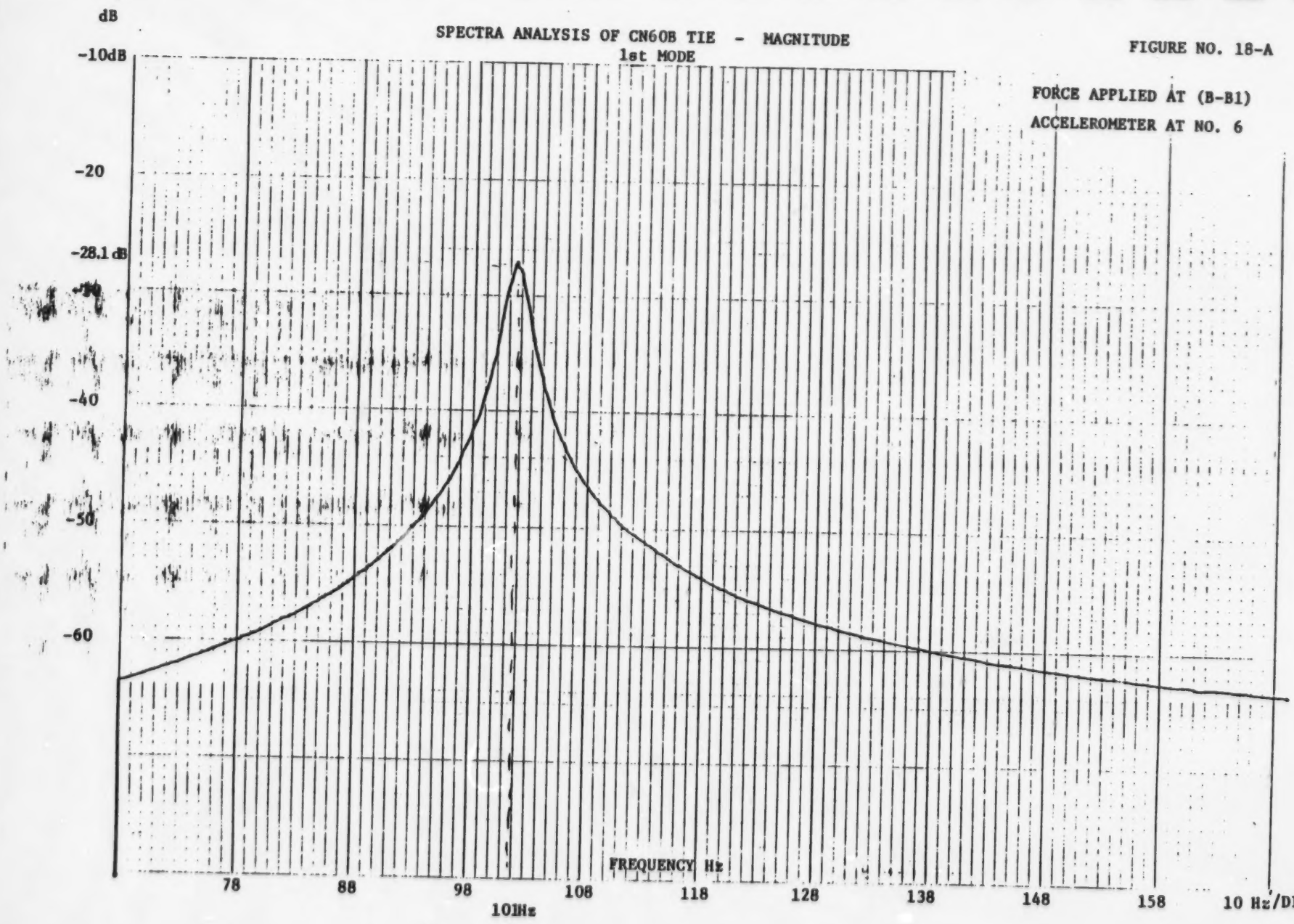
dB
SPECTRA ANALYSIS OF CN60B TIE - MAGNITUDE
1st MODE
FIGURE NO. 18-A
FORCE APPLIED AT (B-B1)
ACCELEROMETER AT NO. 6
-10dB
-20
-28.1 dB
-40
-50
-60
FREQUENCY Hz
78
88
98
101Hz
108
118
128
138
148
158
10 Hz/DIV.

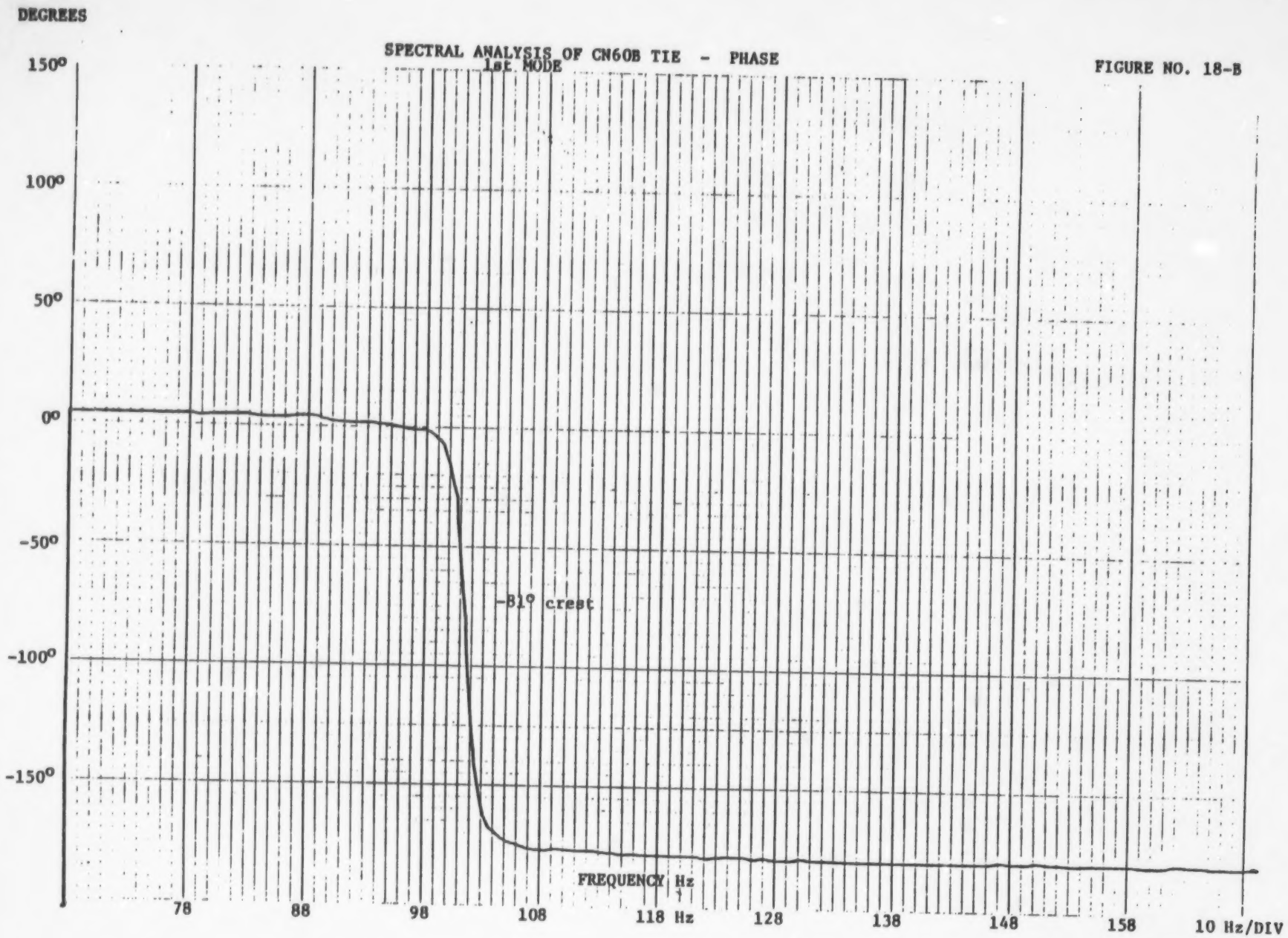
DEGREES
SPECTRAL ANALYSIS OF CN60B TIE - PHASE
1st MODE
FIGURE NO. 18-B
150°
100°
50°
0°
-50°
-100°
-150°
-81° crest
FREQUENCY Hz
78
88
98
108
118 Hz
128
138
148
158
10 Hz/DIV

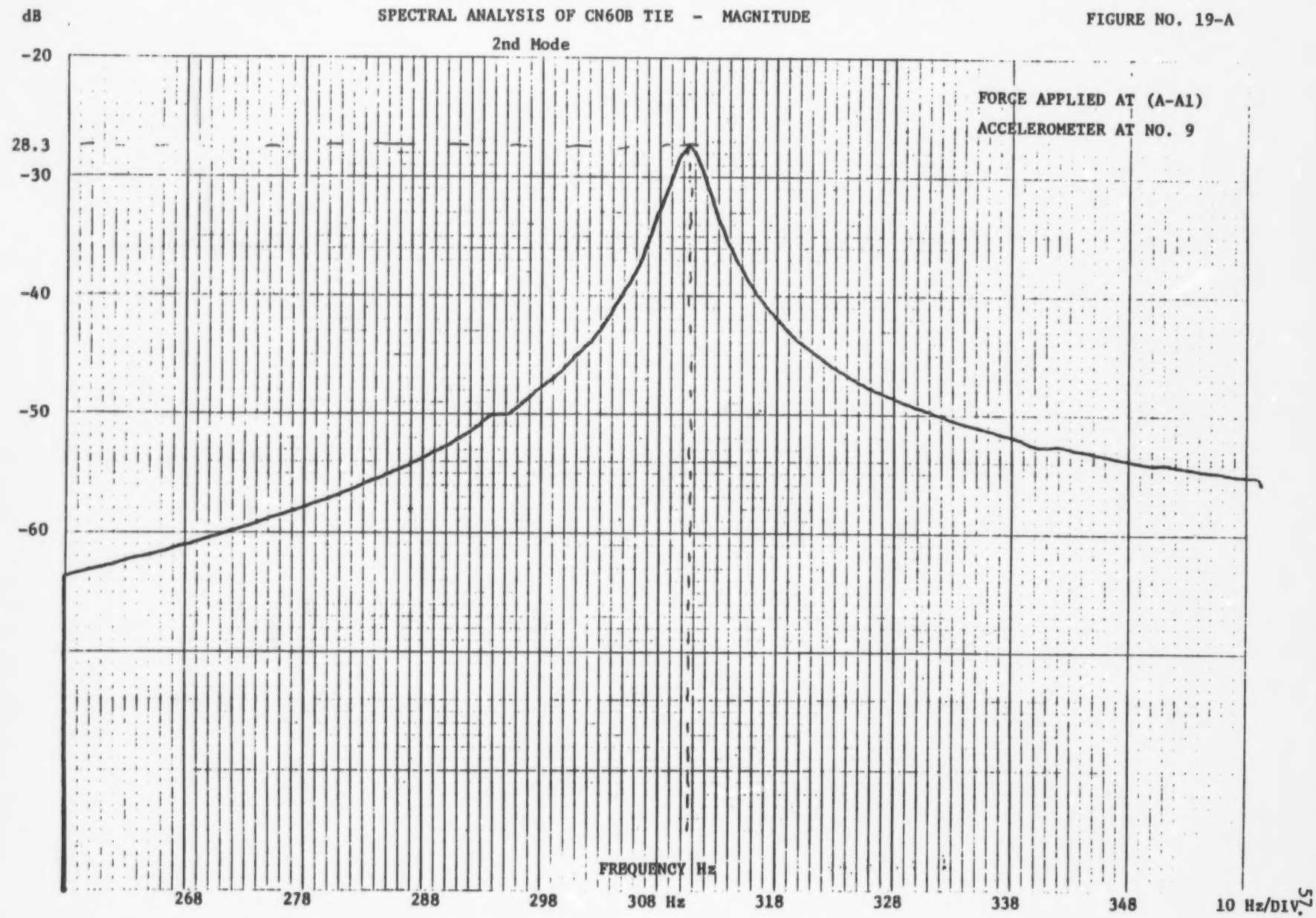
dB
SPECTRAL ANALYSIS OF CN60B TIE - MAGNITUDE
2nd Mode
FIGURE NO. 19-A
-20
28.3
-30
-40
-50
-60
FORCE APPLIED AT (A-A1)
ACCELEROMETER AT NO. 9
FREQUENCY Hz
268
278
288
298
308 Hz
318
328
338
348
10 Hz/DIV.

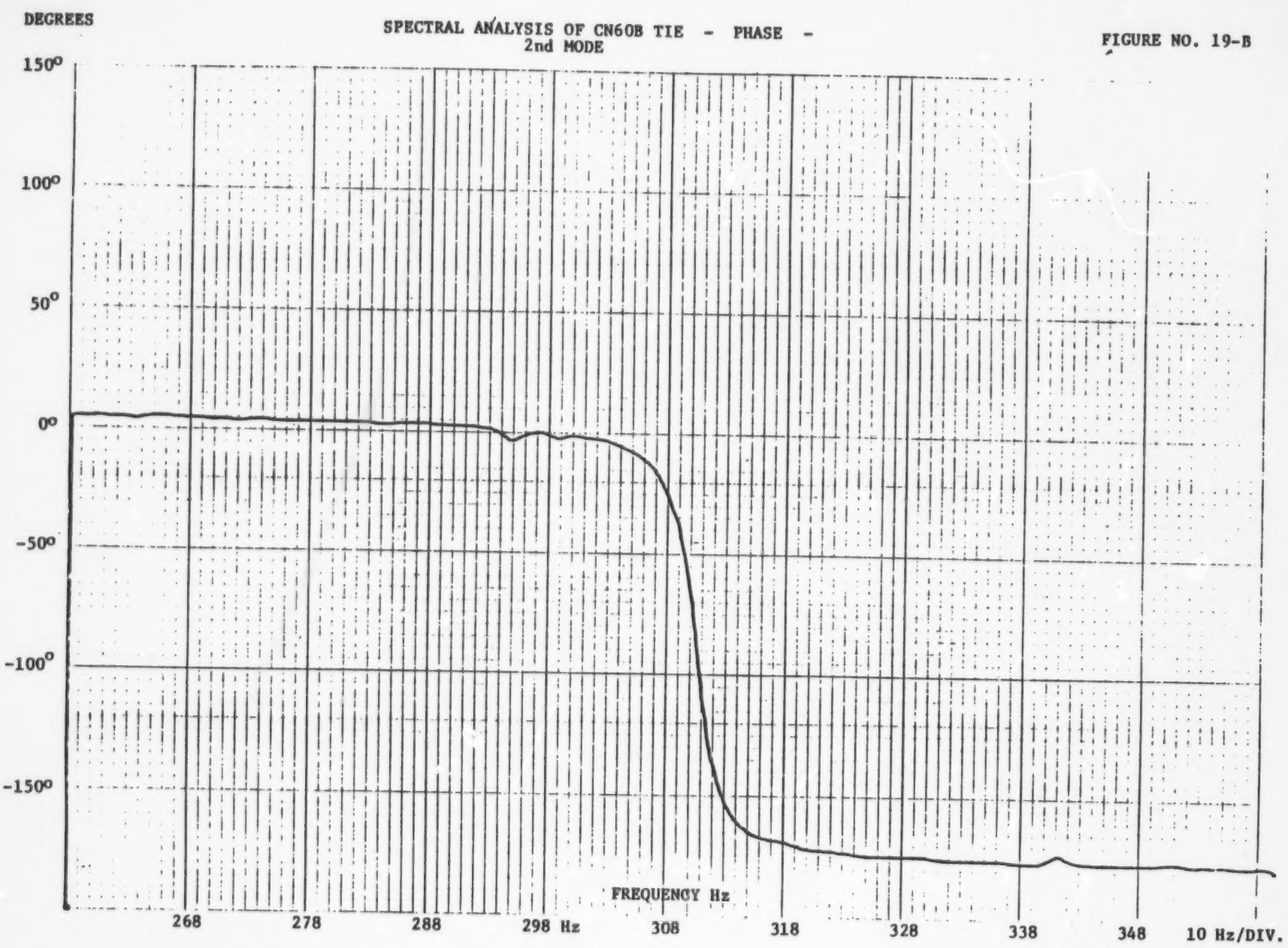
DEGREES
SPECTRAL ANALYSIS OF CN60B TIE - PHASE -
2nd MODE
FIGURE NO. 19-B
150°
100°
50°
0°
-50°
-100°
-150°
FREQUENCY Hz
268
278
288
298 Hz
308
318
328
338
348
10 Hz/DIV.

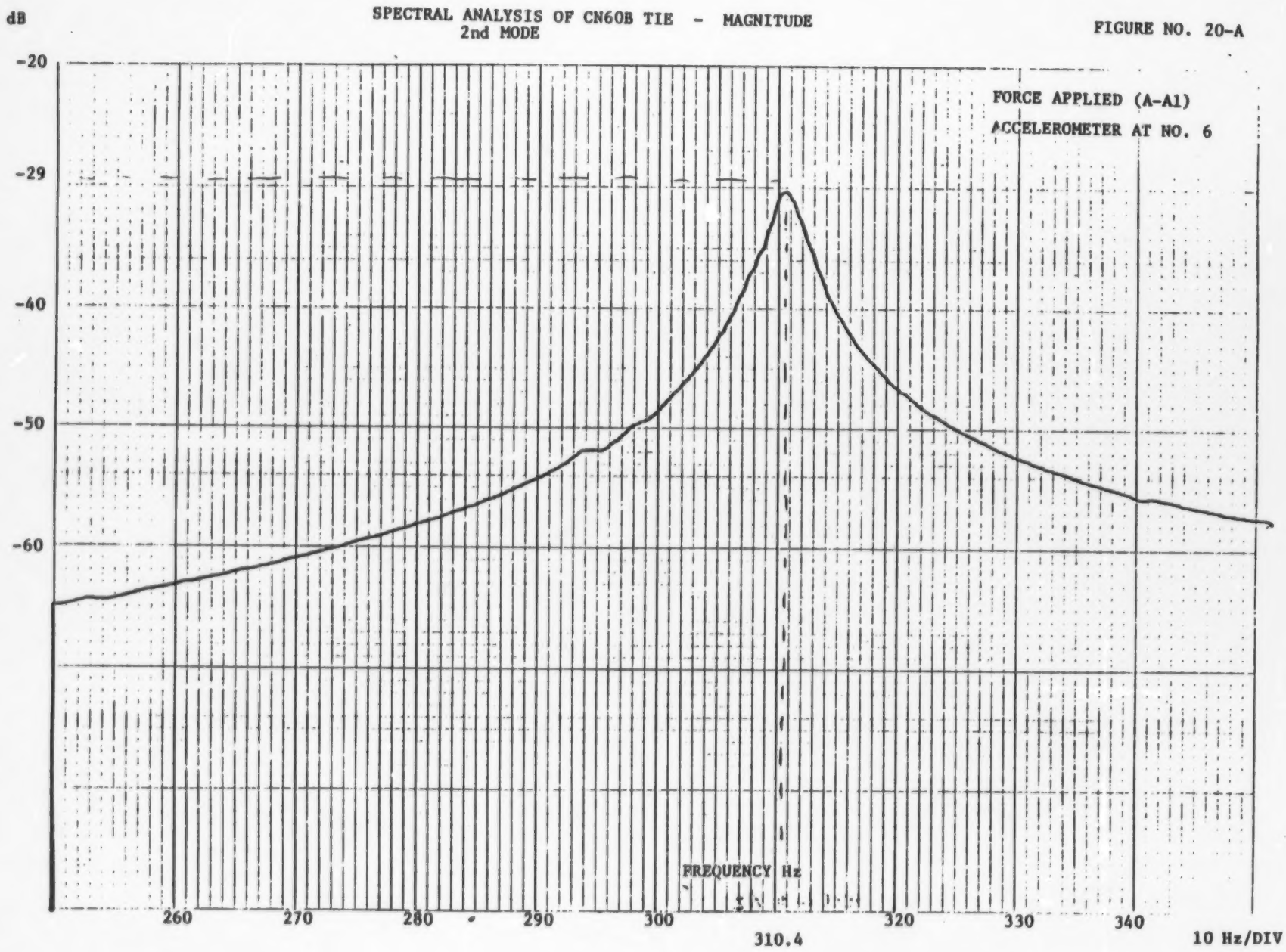
dB
SPECTRAL ANALYSIS OF CN60B TIE - MAGNITUDE
2nd MODE
FIGURE NO. 20-A
FORCE APPLIED (A-A1)
ACCELEROMETER AT NO. 6
-20
-29
-40
-50
-60
FREQUENCY Hz
260
270
280
290
300
310.4
320
330
340
10 Hz/DIV

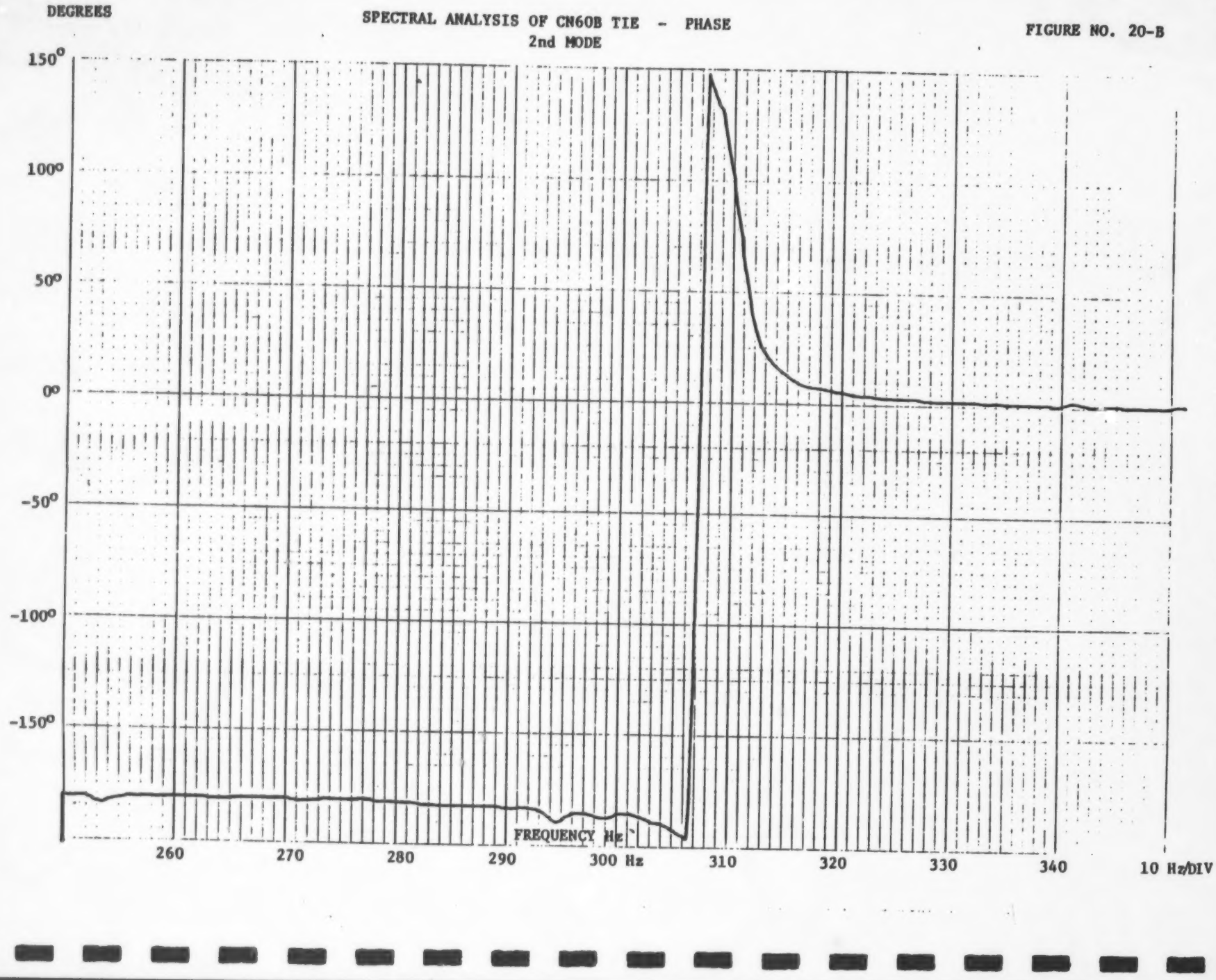
DEGREES
SPECTRAL ANALYSIS OF CN60B TIE - PHASE
2nd MODE
FIGURE NO. 20-B
150°
100°
50°
0°
-50°
-100°
-150°
FREQUENCY Hz
260
270
280
290
300 Hz
310
320
330
340
10 Hz/DIV

SPECTRAL ANALYSIS OF CN60B TIE - MAGNITUDE
3RD MODE

FIGURE NO. 21-A

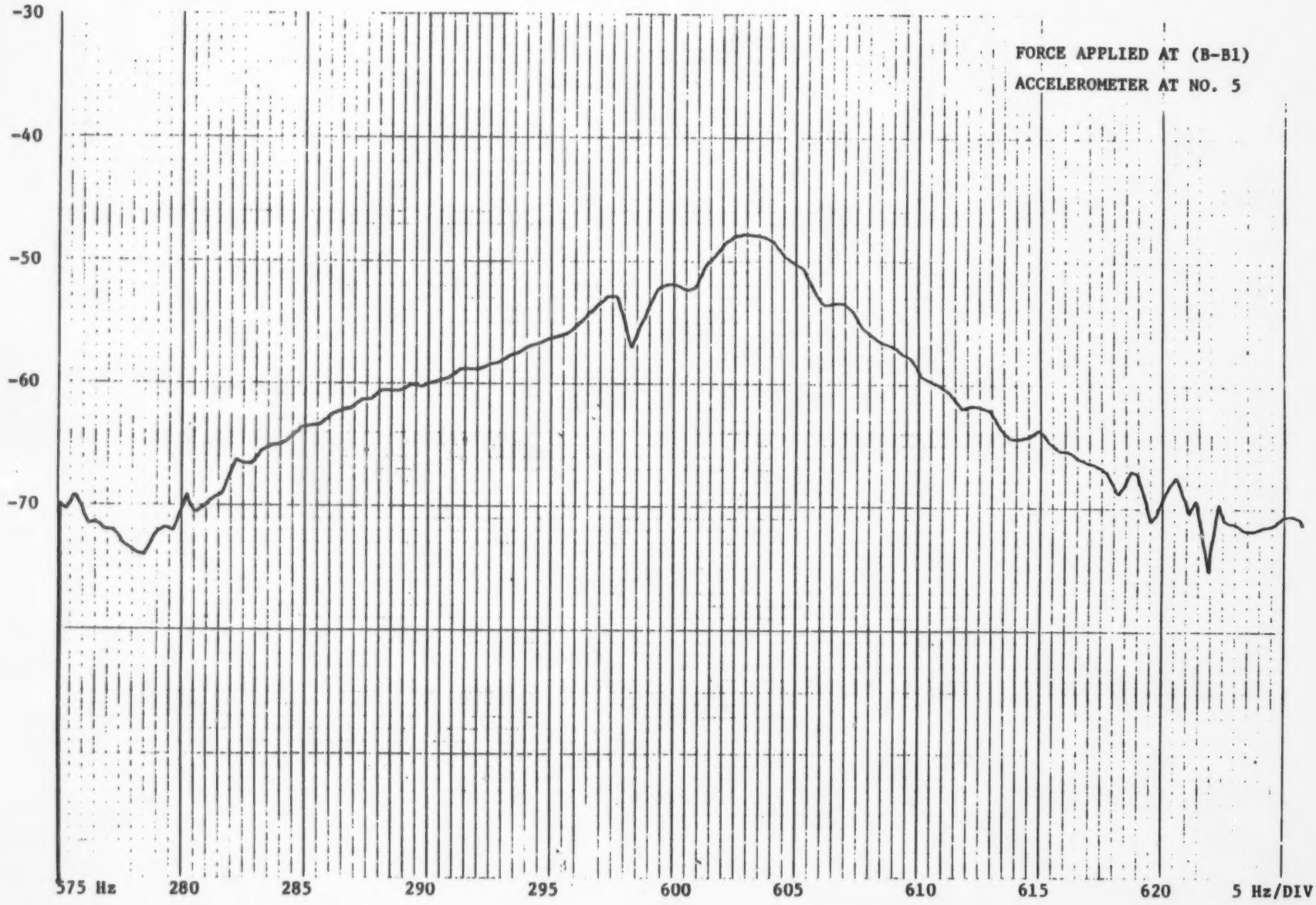

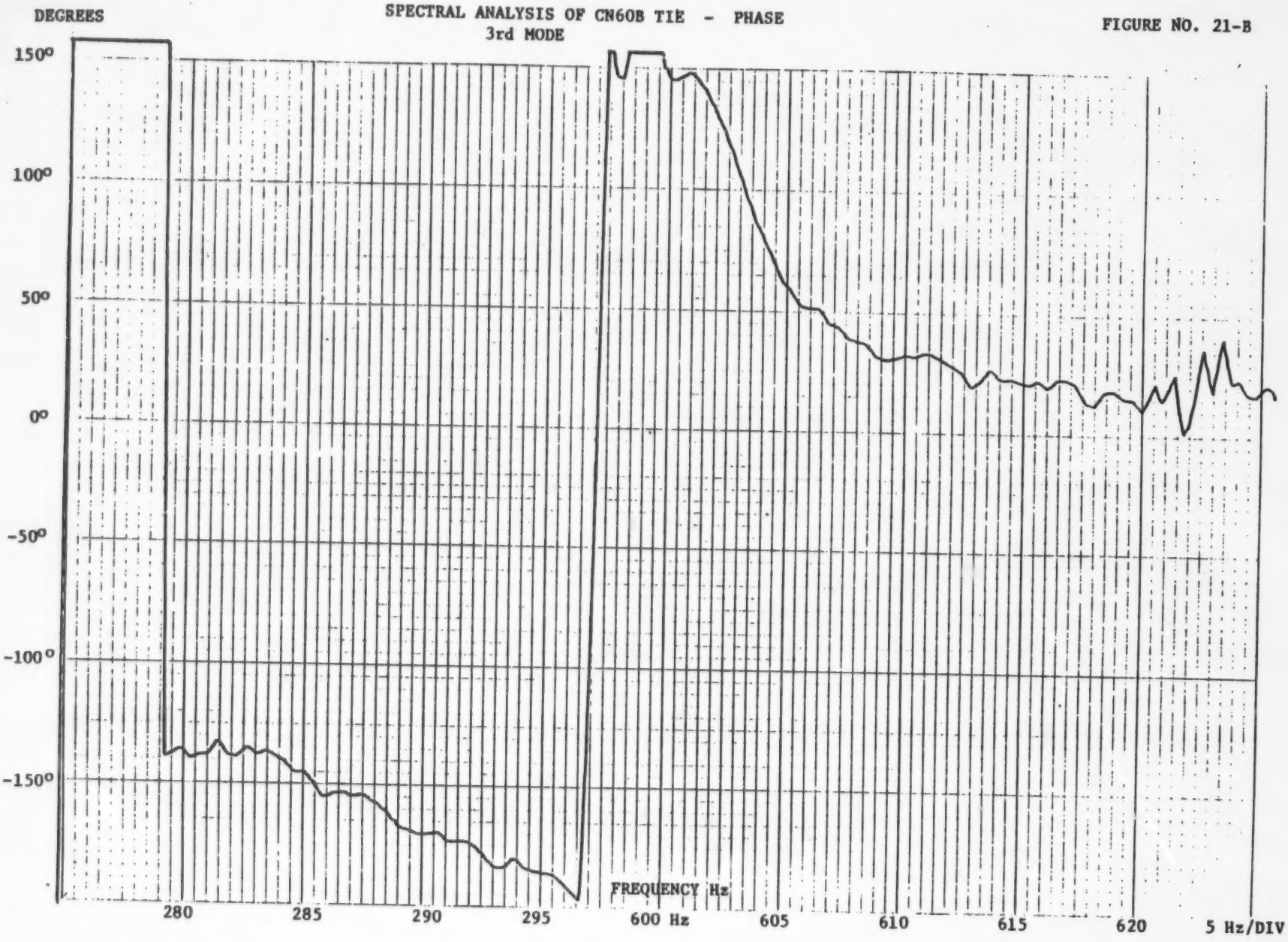
DEGREES
SPECTRAL ANALYSIS OF CN60B TIE - PHASE
3rd MODE
FIGURE NO. 21-B
150°
100°
50°
0°
-50°
-100°
-150°
280
285
290
295
600 Hz
605
610
615
620
FREQUENCY Hz
5 Hz/DIV

SPECTRAL ANALYSIS OF CN60B TIE - MAGNITUDE
3rd MODE

FIGURE NO. 22-A

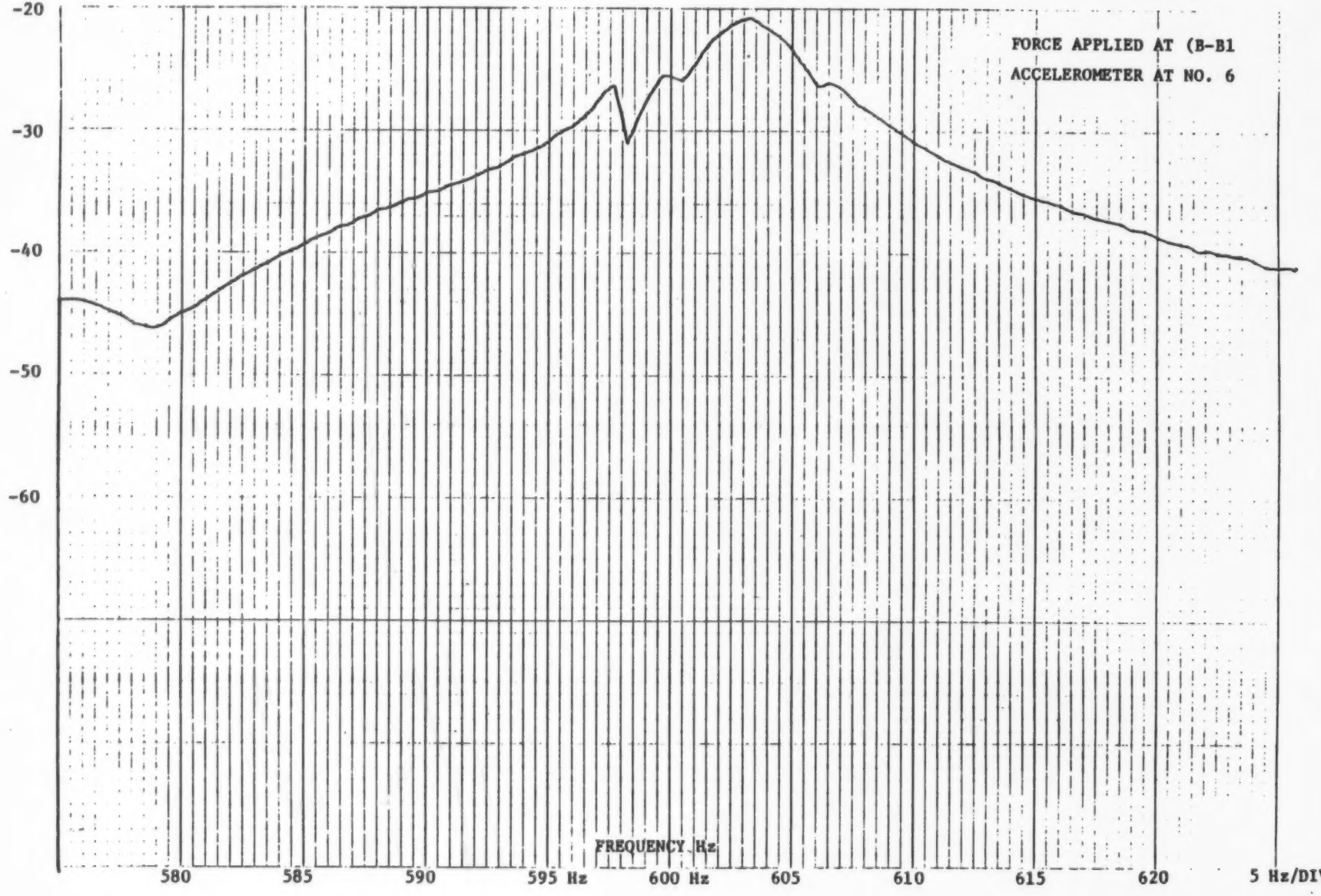

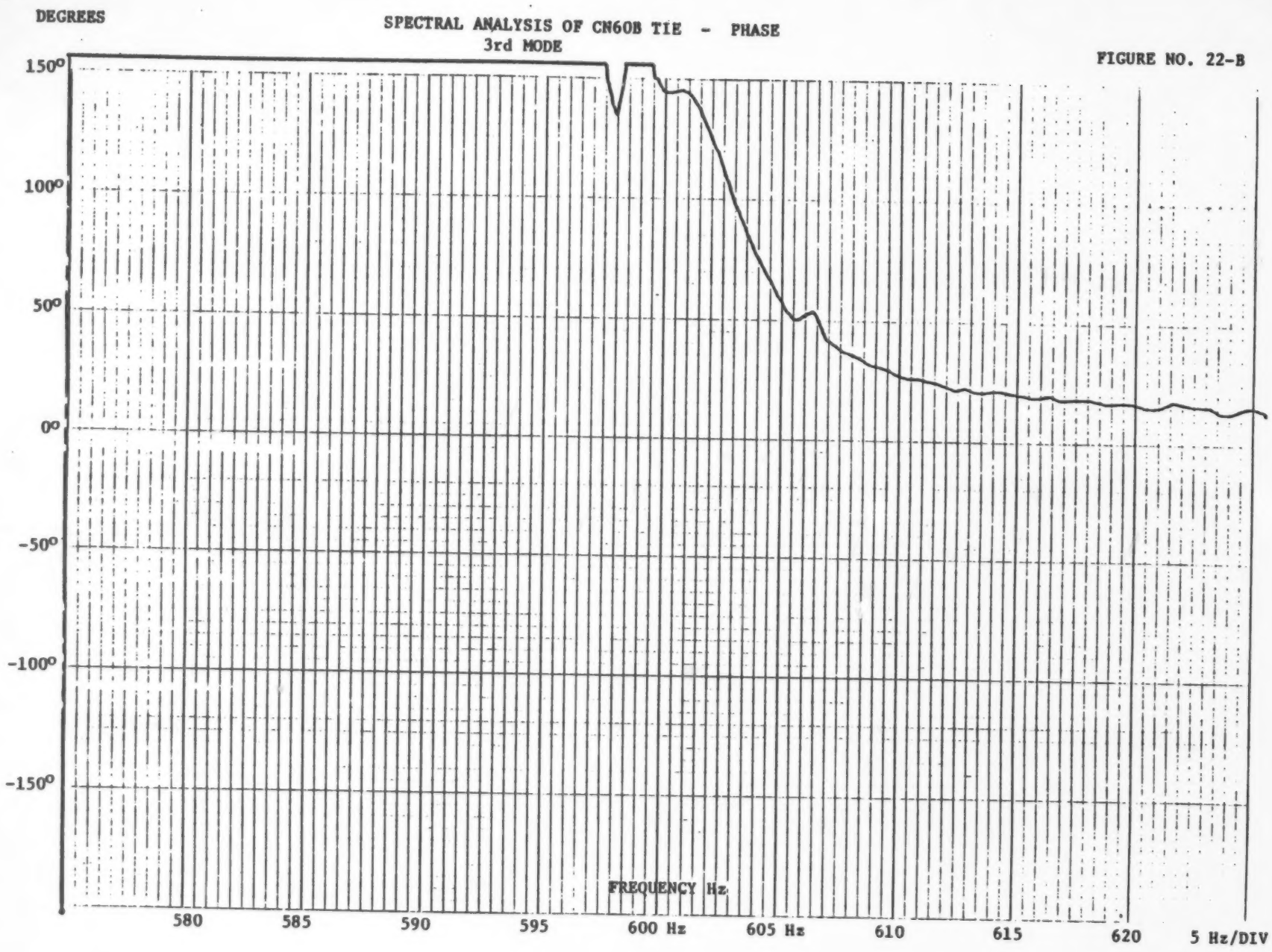
DEGREES
SPECTRAL ANALYSIS OF CN60B TIE - PHASE
3rd MODE
FIGURE NO. 22-B
150°
100°
50°
0°
-50°
-100°
-150°
FREQUENCY Hz
580
585
590
595
600 Hz
605 Hz
610
615
620
5 Hz/DIV

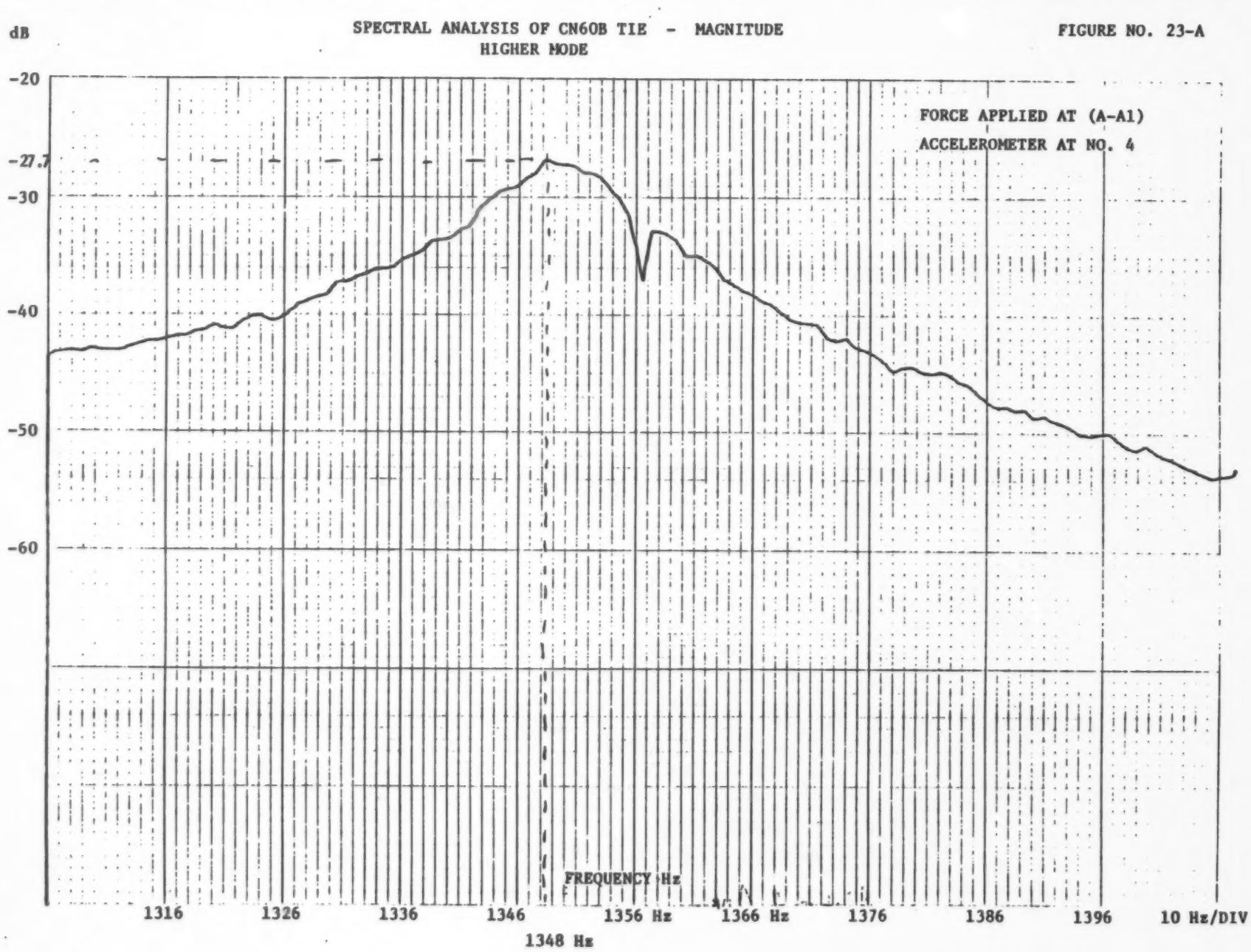
dB
SPECTRAL ANALYSIS OF CN60B TIE - MAGNITUDE
HIGHER MODE
FIGURE NO. 23-A
-20
-27.7
-30
-40
-50
-60
FORCE APPLIED AT (A-A1)
ACCELEROMETER AT NO. 4
FREQUENCY Hz
1316
1326
1336
1346
1348 Hz
1356 Hz
1366 Hz
1376
1386
1396
10 Hz/DIV

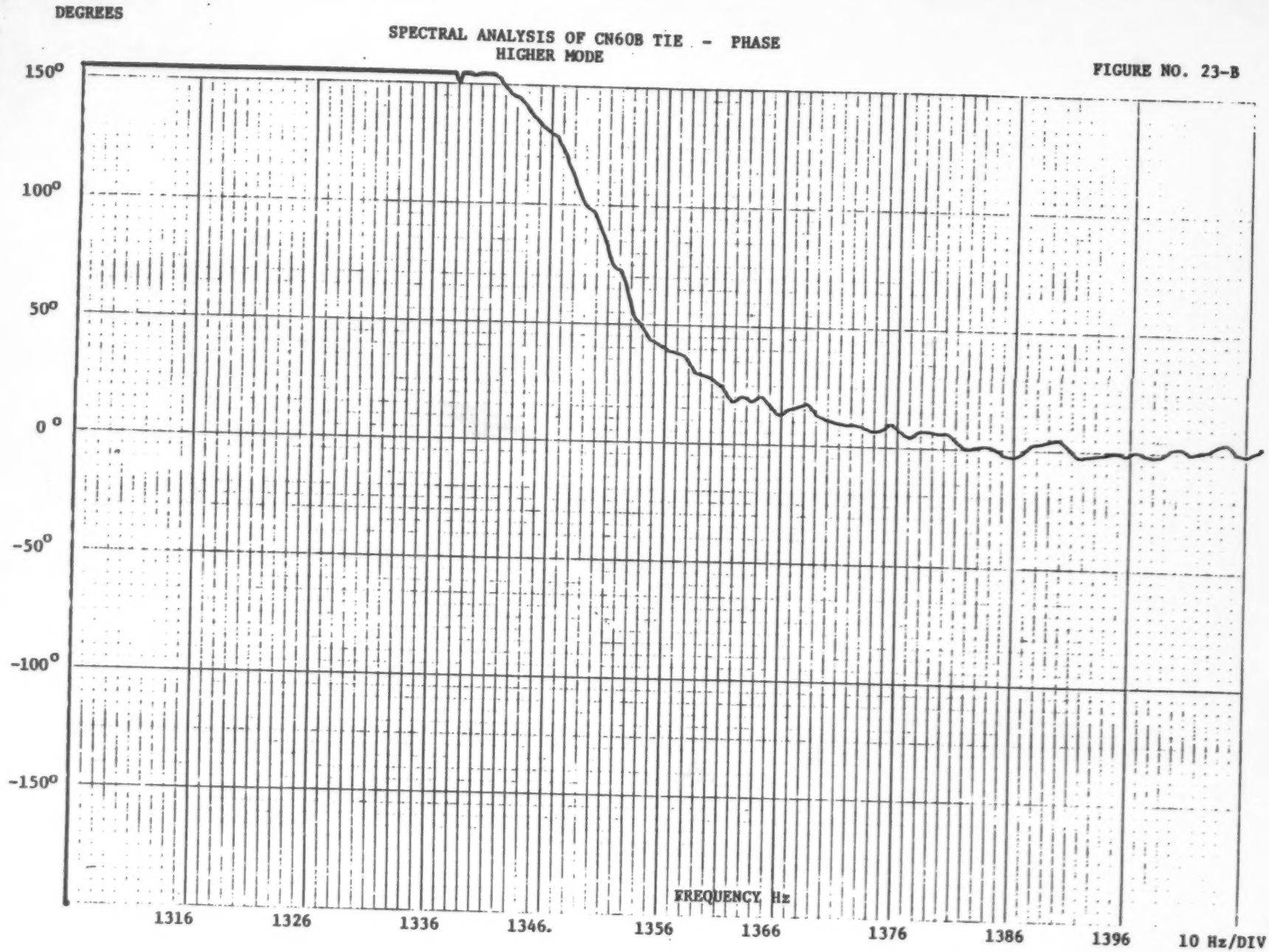
DEGREES
SPECTRAL ANALYSIS OF CN60B TIE - PHASE
HIGHER MODE
FIGURE NO. 23-B
150°
100°
50°
0 °
-50°
-100°
-150°
FREQUENCY Hz
1316
1326
1336
1346.
1356
1366
1376
1386
1396
10 Hz/DIV

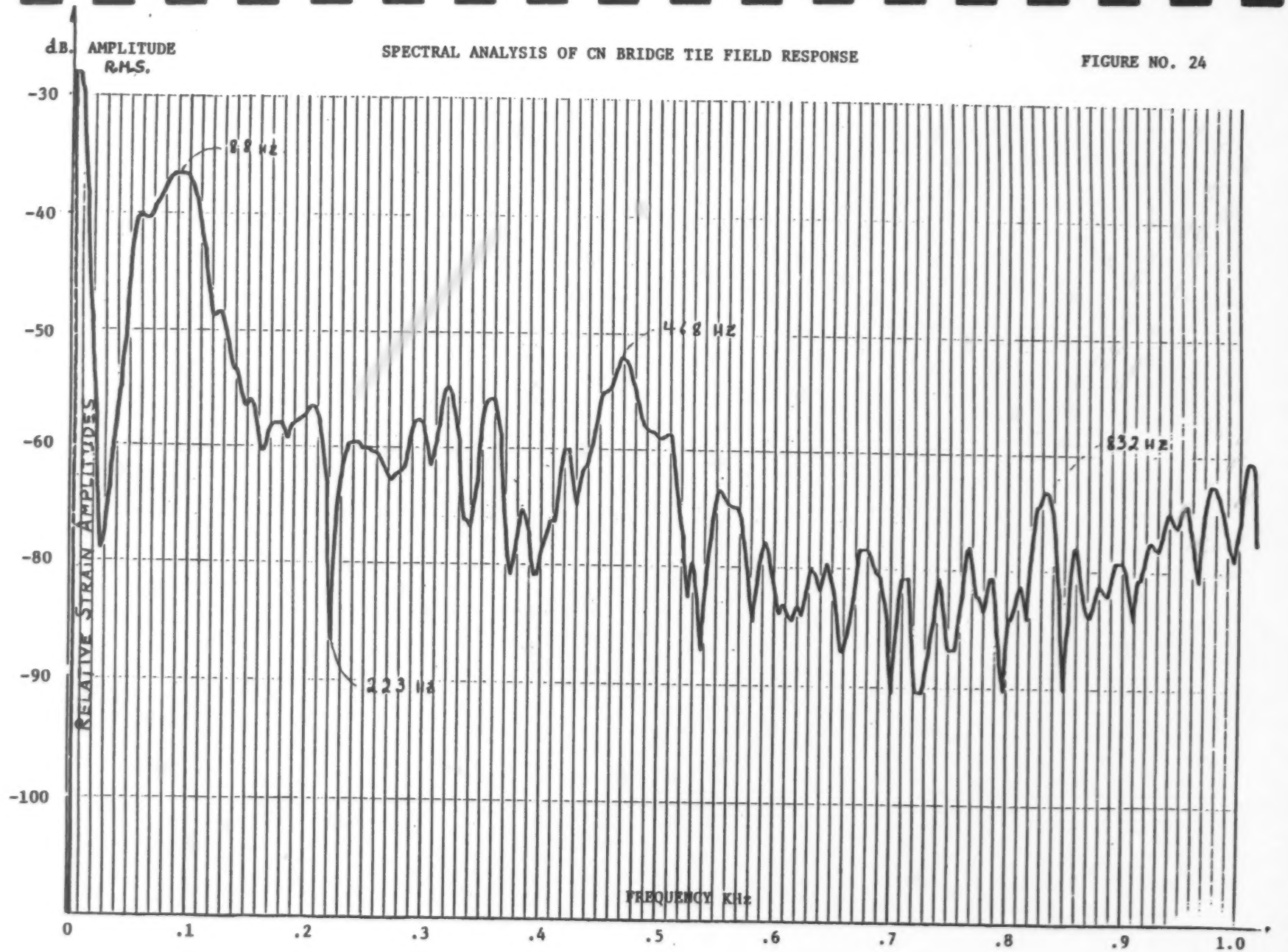
dB. AMPLITUDE R.M.S.
SPECTRAL ANALYSIS OF CN BRIDGE TIE FIELD RESPONSE
FIGURE NO. 24
-30
-40
-50
-60
-80
-90
-100
RELATIVE STRAIN AMPLITUDES
88 Hz
223 Hz
468 Hz
832 Hz
FREQUENCY KHz
0
.1
.2
.3
.4
.5
.6
.7
.8
.9
1.0